

Energetics of Amino Acid Synthesis in Alkaline Hydrothermal Environments

Norio Kitadai

Received: 23 July 2014 / Accepted: 27 January 2015 /

Published online: 22 March 2015

© Springer Science+Business Media Dordrecht 2015

Abstract Alkaline hydrothermal systems have received considerable attention as candidates for the origin and evolution of life on the primitive Earth. Nevertheless, sufficient information has not yet been obtained for the thermodynamic properties of amino acids, which are necessary components for life, at high temperatures and alkaline pH. These properties were estimated using experimental high-temperature volume and heat capacity data reported in the literature for several amino acids, together with correlation algorithms and the revised Helgeson–Kirkham–Flowers (HKF) equations of state. This approach enabled determination of a complete set of the standard molal thermodynamic data and the revised HKF parameters for the 20 protein amino acids in their zwitterionic and ionization states. The obtained dataset was then used to evaluate the energetics of amino acid syntheses from simple inorganic precursors (CO_2 , H_2 , NH_3 and H_2S) in a simulated alkaline hydrothermal system on the Hadean Earth. Results show that mixing between CO_2 -rich seawater and the H_2 -rich hydrothermal fluid can produce energetically favorable conditions for amino acid syntheses, particularly in the lower-temperature region of such systems. Together with data related to the pH and temperature dependences of the energetics of amino acid polymerizations presented in earlier reports, these results suggest the following. Hadean alkaline hydrothermal settings, where steep pH and temperature gradients may have existed between cool, slightly acidic Hadean ocean water and hot, alkaline hydrothermal fluids at the vent–ocean interface, may be energetically the most suitable environment for the synthesis and polymerization of amino acids.

Keywords Abiotic organic synthesis · Origin of life · Prebiotic evolution

Introduction

Since their discovery in the late 1970s, submarine hydrothermal systems have received considerable attention as candidates for the origin and early evolution of life on Earth (e.g., Corliss et al. 1981; Baross and Hoffman 1985; Martin et al. 2008). Hydrothermal vents have been discovered more than 500 sites throughout the oceans (Tivey 2007; Takai and Nakamura

N. Kitadai (✉)

Earth–Life Science Institute, Tokyo Institute of Technology, 2-12-1-IE-1 Ookayama, Meguro-ku, Tokyo
152-8550, Japan
e-mail: nkitadai@elsi.jp

2011). Most are located at seafloor spreading zones, which are directly above magma chambers. Consequently, their effluent comes into direct contact with magma and emerges at the vent–ocean interface with a temperature often exceeding 300 °C. Such ‘black smokers’ are typically acidic (pH 2–3) and are rich in dissolved transition metals such as Fe(II) and Mn(II) (Tivey 2007). A new type of vent system, the Lost City hydrothermal field, was discovered in 2000 more than 15 km from the spreading axis of the Mid-Atlantic Ridge (Kelley et al. 2001, 2005). Unlike vent systems that are located directly on the spreading zone, the water circulating these off-axis vents makes no contact with magma, and emerges at a temperature of around 70–90 °C. Its fluid composition derives from exothermic reactions between seawater and uplifted mantle peridotite, rather than from interactions between seawater and cooling basalts (Martin and Fyfe 1970; Lowell and Rona 2002; Emmanuel and Berkowitz 2006). The peridotite–seawater reactions associated with the oxidation of iron produce alkaline fluids (pH 9–11) that are rich in H₂ and CH₄ and other low-molecular-mass hydrocarbons (Proskurowski et al. 2008; Konn et al. 2009).

Russell and colleagues have proposed that life arose within alkaline hydrothermal vents similar to those of the Lost City (Russell et al. 1994, 2010, 2014; Russell 2003, 2007; Martin and Russell 2007). A proposed beneficial characteristic for life there is the proton gradient at the interface between the alkaline effluent (pH 10–11) and the possibly slightly acidic Hadean ocean (pH 5–6) (Macleod et al. 1994; Morse and Mackenzie 1998). Such proton gradients could have provided a geochemically-generated chemiosmotic potential that may have served as a template upon which biological chemiosmotic gradients evolved if the two were physically separated by a semiporous barrier such as a layer of sulfide minerals at a hydrothermal vent. Alkaline effluent might also provide biologically important heavy metals such as Mo and W because their sulfide species (e.g. MoS₄²⁻) are soluble at alkaline pH, but not at neutral pH (Martin and Russell 2007; Helz et al. 2014). Mo and W are known to catalyze the transfer of O²⁻ from substrate onto water or vice versa (S + H₂O ↔ SO + 2H⁺ + 2e⁻) at the active sites of oxido reductases (Doring and Schulzke 2010). These reactions are part of the carbon, nitrogen and sulfur metabolism and fundamentally important for all organisms (Doring and Schulzke 2010).

One difficulty with this scenario is the instability of ribonucleic acid (RNA) at alkaline pH, which is incompatible with the RNA world hypothesis (Gilbert 1986; Joyce 2002). Hydroxyl groups attack phosphate groups, thereby disrupting the polymeric backbone of the RNA molecule through transesterification reactions (Li and Breaker 1999). High pH also presents problems in terms of the availability of inorganic carbon. High pH results in the precipitation of carbonate minerals and the near complete removal of aqueous inorganic carbon species, leaving few carbon sources that can be fixed into biomass (Schrenk and Brazelton 2013). Consequently, this scenario is not without controversy (Bernhardt and Tate 2012), though it persists as an active topic of study in both field (e.g., Nakamura et al. 2010) and laboratory (e.g., Barge et al. 2014) investigations.

To elucidate the role of alkaline hydrothermal systems in the origin of life on the Hadean Earth, reliable quantitative data must be accumulated to ascertain the reactivity of biomolecules at high temperature and alkaline pH. Thermodynamic calculation is a powerful technique to evaluate the potential for abiotic organic synthesis in aqueous solution. The revised Helgeson–Kirkham–Flowers (HKF) equations of state (Helgeson et al. 1981; Tanger and Helgeson 1988) permit the prediction of thermodynamic properties of aqueous species at temperatures up to 1000 °C and pressures up to 5 kb. To date, the thermodynamic data and the revised HKF parameters for hundreds of aqueous organic species including amino acids have been calculated (summarized in LaRowe and Van Cappellen 2011). They have been used to predict the synthesis and polymerization behaviors of organic species as a function of

temperature, pressure, pH, and redox state (e.g., Shock and Schulte 1998; Amend and McCollom 2009).

Amino acids are building blocks of proteins, which are fundamental to life as we know it. Nonetheless, the revised HKF equations of state have not yet been applied to evaluate the thermodynamic behaviors of amino acids under alkaline hydrothermal conditions ($\text{pH} > 9$) (Shock 1992; Amend and Shock 1998; Shock and Canovas 2010) because the revised HKF parameters for negatively ionized amino acids, which are the dominant species under alkaline pH, have not been calculated except for a few amino acids (Gly^- , Kitadai 2014; Arg^- and Lys^- , Dick et al. 2006). These calculations had been limited by the dearth of experimental high-temperature volume, heat capacity and compressibility data (>100 °C) of the negatively-charged amino acid species. Since 2001, however, the standard molal volume and heat capacity of ionization ($\Delta_i V^\circ$ and $\Delta_i C_P^\circ$, respectively) of various amino acids (Ala, Asp, Glu, Gly, His, Ile, Met, Pro, Ser, Thr, and Val) have been measured experimentally by Woolley and co-workers as a function of temperature from 5 to 120 °C at 0.35 MPa (Jardine et al. 2001; Price et al. 2003a,b; Sorenson et al. 2003; Ziemer et al. 2006a,b,c; Ziemer and Woolley 2007a,b,c). These values, together with the reported standard molal thermodynamic data at 25 °C and 1 bar, along with the revised HKF parameters for the zwitterionic amino acids (Dick et al. 2006), are useful for calculating several revised HKF parameters (c_1 , c_2 , σ , ξ and ω ; see Appendix A) for the negatively charged and positively charged amino acid species, respectively. Although indeterminable parameters (a_1 , a_2 , a_3 , and a_4) remain because of the paucity of experimental compressibility data, these can be estimated based on correlation algorithms developed by Amend and Helgeson (1997, 2000) and by Dick et al. (2006). The revised HKF parameters for other amino acids in various ionization states are also generable using the correlation algorithms in combination with the dataset obtained through the foregoing procedures.

In this study, a full set of the revised HKF parameters for the 20 protein amino acids in their zwitterionic, negative and positive ionization states is presented. The obtained parameters enable calculation of the thermodynamic behaviors of the 20 coded biological amino acids over widely diverse temperatures and pH values. As a test to evaluate whether or not an alkaline hydrothermal system is favorable for the abiotic synthesis of amino acids, the Gibbs energies necessary to synthesize the 20 protein amino acids from simple inorganic precursors (CO_2 , H_2 , NH_3 , and H_2S) under simulated alkaline hydrothermal system conditions on the Hadean Earth were calculated. Based on the results, together with the temperature and pH dependences of the energetics of amino acid polymerizations revealed in the foregoing paper by Kitadai (2014), the suitability of alkaline hydrothermal systems for the synthesis and polymerization of amino acids is discussed.

Calculation Methodology

The thermodynamic data and revised HKF parameters for the 20 protein amino acids in their zwitterionic and ionized states were obtained as described below. The revised HKF equations of state and the thermodynamic conventions adopted for this study are summarized in Appendix A.

Standard Molal Thermodynamic Data for the 20 Protein Amino Acids at 25 °C and 1 bar

Table 1 presents values of the standard molal Gibbs energy ($\Delta_f G^\circ$), enthalpy ($\Delta_f H^\circ$) and entropy (S°) at 25 °C and 1 bar for the 20 protein amino acids. The values for the zwitterionic

Table 1 Standard molal thermodynamic data at 25 °C and 1 bar and revised HKF equation of state parameters for 20 protein amino acids in their zwitterionic and ionization states^a kcal mol⁻¹, ^b cal mol⁻¹ K⁻¹, ^c cm³ mol⁻¹, ^d cal mol⁻¹ bar⁻¹, ^e cal mol⁻¹, ^f cal K mol⁻¹ bar⁻¹, ^g cal K mol⁻¹, ^h Dick et al. (2006), ⁱ Kitadai (2014), ^j LaKowe and Dick (2012), ^k Ziemer et al. (2006c), ^l Smith and Marcell (2004), ^m Nagai et al. (2008), ⁿ Ziemer and Woolley (2007c), ^o Hamborg et al. (2007), ^p Goldberg et al. (2002), ^q Price et al. (2003a), ^r Ziemer and Woolley (2007a), ^s Ziemer and Woolley (2007b), ^t Sorenson et al. (2003), ^u Ziemer et al. (2006b), ^v Price et al. (2003b), ^w Kochergina et al. (2011), ^x Kochergina et al. (2013), ^y calculated from the values of $\Delta_f G^\circ$ and $\Delta_f H^\circ$ given in this table using values of S° for elements taken from Cox et al. (1989)

Species	$\Delta_f G^\circ$	$\Delta_f H^\circ$	S°	C_p°	V°	$a_1^d \times 10$	$a_2^e \times 10^{-2}$	a_3^f	$a_4^g \times 10^{-4}$	c_l^b	$c_2^h \times 10^{-4}$	$\omega^i \times 10^{-5}$
Ala [±]	-88.81 ^h	-132.50 ^h	38.83 ^h	33.6 ^h	60.4 ^h	14.90 ^h	1.74 ^h	7.16 ^h	-3.69 ^h	49.5 ^h	-7.00 ^h	0.18 ^h
Ala ⁺	-92.00 ^k	-133.20 ^k	47.18 ^y	64.5	67.9	20.02	-6.38	-7.07	-0.88	61.6	0.46	-0.21
Ala ⁻	-75.36 ^k	-121.59 ^k	30.30 ^y	18.0	59.5	12.55	4.99	18.91	-5.78	28.9	-5.87	-0.32
Arg [±]	-57.36 ^h	-143.06 ^h	80.06 ^h	67.4 ^h	123.9 ^h	28.83 ^h	8.21 ^h	7.20 ^h	-5.95 ^h	94.8 ^h	-12.50 ^h	0.22 ^h
Arg ⁺	-69.63 ^l	-153.86 ^l	84.98 ^h	77.6 ^h	122.5 ^h	31.72 ^h	0.22 ^h	5.46 ^h	-5.15 ^h	103.8 ^h	-9.60 ^h	0.73 ^h
Arg ⁻	-41.07 ^m	-142.65 ^m	26.82 ^y	81.1 ^h	143.0 ^h	31.28 ^h	13.76 ^h	32.12 ^h	-9.94 ^h	141.9 ^h	-19.60 ^h	2.30 ^h
Arg ^{±+}	-72.11 ^l	-154.86 ^l	89.96 ^y	105.5	132.6	38.92	-8.28	-15.70	-2.21	120.3	-3.25	0.90
Asn [±]	-125.49 ^h	-182.70 ^h	57.88 ^h	30.8 ^h	77.4 ^h	19.83 ^h	2.37 ^h	3.76 ^h	-4.81 ^h	56.5 ^h	-11.70 ^h	0.21 ^h
Asn ⁺	-128.44 ^w	-183.63 ^w	64.65 ^y	60.7	85.7	24.64	-4.50	-4.58	-2.24	68.0	0.06	0.81
Asn ⁻	-113.25 ^w	-172.96 ^w	49.51 ^y	16.5	77.1	17.80	6.85	23.16	-7.12	44.6	-4.36	2.10
Asp [±]	-172.51 ^h	-226.34 ^h	55.22 ^h	32.4 ^h	74.7 ^h	18.96 ^h	3.05 ^h	-6.62 ^h	-2.23 ^h	58.1 ^h	-11.90 ^h	0.17 ^h
Asp ⁺	-175.17 ⁿ	-227.97 ⁿ	58.68 ^y	58.1	84.9	22.74	-4.58	0.19	-2.18	58.9	-3.66	-0.73
Asp ⁻	-167.38 ⁿ	-225.18 ⁿ	41.90 ^y	2.7 ^h	64.8 ^h	16.96 ^h	5.77 ^h	10.11 ^h	-6.37 ^h	56.3 ^h	-15.30 ^h	2.47 ^h
Asp ^{±-}	-153.52 ^o	-215.33 ^o	28.43 ^y	-9.9	64.8	15.19	9.10	23.54	-8.14	44.4	-12.45	3.16
Cys [±]	-80.33 ^h	-124.07 ^h	46.32 ^h	47.1 ^h	73.5 ^h	18.14 ^h	2.40 ^h	9.31 ^h	-4.97 ^h	59.8 ^h	-5.60 ^h	0.15 ^h
Cys ⁺	-82.66 ^p	-123.93 ^p	54.63 ^y	76.3	81.7	22.85	-4.92	2.05	-1.93	71.6	6.86	1.01
Cys ⁻	-68.92 ^h	-115.44 ^h	37.01 ^y	18.1 ^h	60.6 ^h	14.44 ^h	5.08 ^h	12.24 ^h	-3.68 ^h	61.0 ^h	-9.50 ^h	2.59 ^h
Cys ^{±-}	-54.25 ^p	-107.29 ^p	15.16 ^y	4.6	60.7	12.26	8.67	37.49	-7.83	49.6	-7.55	3.23
Gln [±]	-126.28 ^h	-191.86 ^h	62.41 ^h	43.8 ^h	93.7 ^h	23.22 ^h	3.58 ^h	5.44 ^h	-5.23 ^h	68.6 ^h	-11.40 ^h	0.18 ^h
Gln ⁺	-129.24 ^s	-192.54 ^s	70.05 ^y	73.1	102.7	28.42	-2.72	-2.17	-3.52	81.4	0.02	0.90
Gln ⁻	-113.72 ^s	-182.18 ^s	52.75 ^y	28.7	93.1	21.44	8.52	24.95	-8.33	58.0	-4.48	2.19
Glu [±]	-173.05 ^h	-234.82 ^h	61.20 ^h	43.5 ^h	90.2 ^h	22.30 ^h	4.23 ^h	6.55 ^h	-5.84 ^h	65.2 ^h	-10.00 ^h	0.15 ^h

Table 1 (continued)

Species	ΔG^{oa}	ΔF^{oa}	$S^o_{Pr, Tr}$	C_p^{ob}	f^{oc}	$a_l \times 10$	$a_2 \times 10^{-2}$	a_3^f	$a_4 \times 10^{-4}$	c_l^b	$c_2 \times 10^{-4}$	$\omega^e \times 10^{-5}$
Glu ⁺	-176.05 ⁿ	-235.70 ⁿ	68.31 ^y	65.7	98.1	25.66	-3.20	-5.05	-3.17	54.4	-4.36	-2.20
Glu ⁻	-167.25 ⁿ	-233.86 ⁿ	44.97 ^y	7.6 ^b	80.0 ^b	20.49 ^b	6.96 ^b	10.86 ^b	-7.02 ^b	47.6 ^b	-7.80 ^b	2.65 ^h
Glu ²⁻	-153.65 ^o	-224.90 ^o	29.42 ^y	-5.3	79.7	19.02	10.67	22.11	-9.27	34.8	-5.11	3.24
Gly ⁺	-88.62 ⁱ	-122.83 ⁱ	37.89 ⁱ	9.3 ^b	43.2 ^b	11.30 ^b	0.71 ^b	3.99 ^b	-3.04 ^b	28.5 ^b	-8.40 ^b	0.23 ^h
Gly ⁻	-91.82 ⁱ	-123.79 ⁱ	45.44 ⁱ	39.7 ⁱ	49.9 ⁱ	15.57 ⁱ	-8.26 ⁱ	-6.62 ⁱ	0.47 ⁱ	39.5 ⁱ	-1.21 ⁱ	-0.33 ⁱ
Gly ⁻	-75.27 ^j	-112.27 ^j	28.57 ^j	-0.8 ⁱ	45.7 ⁱ	9.76 ⁱ	3.54 ⁱ	19.85 ⁱ	-4.73 ⁱ	21.6 ⁱ	-7.92 ⁱ	0.69 ^j
His [±]	-48.42 ^h	-108.20 ^h	66.00 ^h	56.2 ^h	99.3 ^h	24.32 ^h	4.80 ^h	7.52 ^h	-6.05 ^h	81.6 ^h	-11.30 ^h	0.27 ^h
His ⁺	-56.57 ^l	-115.30 ^l	69.50 ^l	59.1 ^h	97.0 ^b	26.64 ^h	-3.40 ^h	-0.88 ^h	-3.07 ^h	88.0 ^h	-12.00 ^h	0.50 ^h
His ⁻	-35.76 ^l	-97.70 ^l	58.75 ^y	37.9	97.7	21.36	9.00	25.83	-8.67	61.9	-7.79	0.62
His ²⁺	-58.75 ^l	-116.30 ^l	73.47 ^y	87.8	106.1	32.48	-11.06	-16.13	-0.21	102.9	-4.28	0.69
Ile [±]	-81.99 ^h	-151.60 ^h	49.70 ^h	91.6 ^h	105.8 ^h	24.49 ^h	6.55 ^h	18.16 ^h	-7.76 ^h	99.7 ^h	-3.60 ^h	0.09 ^h
Ile ⁺	-85.19 ^f	-151.83 ^f	59.64 ^y	120.5	115.1	31.68	-1.42	-6.57	-4.46	121.0	1.49	0.39
Ile ⁻	-68.75 ^f	-140.69 ^f	41.92 ^y	77.6	106.1	24.15	9.89	21.15	-9.31	96.0	-4.9	0.75
Leu [±]	-84.20 ^h	-153.60 ^h	50.41 ^h	95.2 ^h	107.8 ^h	24.68 ^h	7.51 ^h	19.93 ^h	-8.37 ^h	102.7 ^h	-3.30 ^h	0.09 ^h
Leu ⁺	-87.38 ^l	-153.99 ^l	59.75 ^y	122.4	117.3	31.28	-1.18	3.94	-4.63	119.1	7.09	1.22
Leu ⁻	-70.91 ^l	-142.75 ^l	42.22 ^y	77.0	106.9	24.18	9.97	30.41	-9.37	95.5	2.20	2.51
Lys [±]	-80.68 ^h	-159.33 ^h	57.91 ^h	63.8 ^h	108.6 ^h	24.56 ^h	8.30 ^h	24.43 ^h	-9.53 ^h	86.6 ^h	-10.90 ^h	0.07 ^h
Lys ⁺	-93.08 ^m	-168.72 ^m	68.00 ^y	67.9 ^h	107.5 ^h	28.62 ^h	-1.51 ^h	4.47 ^h	-3.99 ^h	95.2 ^h	-8.00 ^h	1.21 ^h
Lys ⁻	-65.81 ^m	-148.95 ^m	42.87 ^y	72.8 ^h	112.2 ^h	28.29 ^h	10.53 ^h	2.97 ^h	-7.61 ^h	133.7 ^h	-18.00 ^h	2.67 ^h
Lys ²⁺	-95.61 ^m	-168.80 ^m	76.20 ^y	96.2	117.0	35.18	-9.91	-13.36	-1.03	110.8	-0.83	1.41
Met [±]	-76.96 ^l	-135.21 ^l	62.81 ^l	70.7 ^h	105.4 ^h	24.95 ^h	6.90 ^h	13.59 ^h	-7.77 ^h	85.3 ^h	-6.60 ^h	0.13 ^h
Met ⁺	-80.0 ^s	-135.51 ^s	72.13 ^y	95.1	114.4	30.54	-1.48	-3.31	-4.41	90.2	0.61	-0.40
Met ⁻	-64.41 ^s	-124.84 ^s	55.51 ^y	51.8	105.7	24.39	9.85	19.31	-9.28	77.2	-7.41	0.87
Phe [±]	-49.43 ^h	-108.90 ^h	56.60 ^h	93.8 ^h	122.1 ^h	28.27 ^h	8.80 ^h	19.34 ^h	-9.38 ^h	108.1 ^h	-6.50 ^h	0.12 ^h
Phe ⁺	-52.43 ^l	-109.50 ^l	64.65 ^y	121.0	132.2	35.42	0.38	-0.44	-5.75	125.1	3.12	1.13

Table 1 (continued)

Species	ΔG^{oa}	ΔF^{oa}	$S^o_{Pr, Tr}$	C_p^{ob}	f^{oc}	$a_l^d \times 10$	$a_2^c \times 10^{-2}$	a_3^f	$a_4^g \times 10^{-4}$	c_l^b	$c_2^E \times 10^{-4}$	$\omega^e \times 10^{-5}$
Phe ⁻	-36.73 ^l	-98.20 ^l	49.89 ^y	75.7	120.9	28.15	11.44	25.73	-10.43	101.5	-1.74	2.42
Pro ⁺	-73.56 ^b	-124.10 ^b	49.83 ^b	43.0 ^h	82.6 ^b	19.39 ^h	4.87 ^b	11.88 ^b	-5.68 ^b	63.6 ^b	-9.50 ^b	0.14 ^h
Pro ⁺	-76.22 ^l	-124.44 ^l	57.61 ^y	73.0	88.5	24.19	-4.21	-4.18	-2.45	70.1	-2.05	-0.77
Pro ⁻	-59.04 ^l	-113.79 ^l	35.72 ^y	40.8	82.9	16.94	7.45	32.30	-7.55	59.9	-5.41	0.70
Ser ⁺	-123.93 ^b	-172.42 ^b	47.24 ^b	27.8 ^b	60.6 ^b	15.69 ^h	0.73 ^h	3.87 ^b	-3.49 ^b	48.5 ^b	-9.40 ^b	0.18 ^h
Ser ⁺	-126.91 ^a	-173.74 ^a	52.82 ^y	58.7	68.5	19.13	-6.30	-2.53	-0.94	56.3	-2.52	-0.82
Ser ⁻	-111.37 ^a	-162.07 ^a	39.82 ^y	12.3	60.4	13.15	5.09	19.39	-5.85	37.1	-9.20	0.35
Thr ⁺	-119.83 ^b	-178.94 ^b	44.23 ^b	50.1 ^h	77.6 ^b	18.94 ^h	2.83 ^b	8.87 ^b	-4.87 ^b	65.5 ^b	-7.10 ^b	0.11 ^h
Thr ⁺	-122.91 ^r	-179.82 ^r	51.61 ^y	78.4	86.1	23.15	-4.46	0.49	-2.27	77.2	-1.57	-0.48
Thr ⁻	-107.33 ^r	-169.02 ^r	35.59 ^y	34.7	75.8	15.31	6.71	27.60	-7.02	46.9	-6.02	-0.22
Trp ⁺	-26.82 ^b	-97.59 ^b	59.96 ^b	99.6 ^b	143.6 ^b	35.91 ^h	9.21 ^h	14.78 ^b	-9.36 ^b	116.8 ^b	-7.80 ^b	0.15 ^h
Trp ⁺	-30.05 ^l	-97.52 ^l	71.04 ^y	126.6	154.5	41.24	2.72	-4.16	-7.44	134.7	0.62	1.02
Trp ⁻	-14.05 ^l	-86.88 ^l	42.99 ^y	81.1	141.9	33.75	13.65	21.44	-12.02	111.0	-4.28	2.31
Tyr ⁺	-91.80 ^b	-157.74 ^b	59.41 ^b	80.2 ^h	124.5 ^h	30.06 ^h	8.49 ^h	8.36 ^b	-8.58 ^h	106.2 ^h	-12.40 ^h	0.09 ^h
Tyr ⁺	-94.58 ^l	-157.40 ^l	69.88 ^y	108.0	134.7	37.25	0.64	-8.74	-5.94	123.0	-1.88	1.22
Tyr ⁻	-79.40 ^l	-148.09 ^l	50.19 ^y	51.2 ^h	111.8 ^h	26.34 ^h	10.49 ^h	16.42 ^h	-7.59 ^h	109.0 ^h	-16.00 ^h	2.78 ^h
Tyr ²⁻	-64.82 ^l	-136.74 ^l	39.35 ^y	15.3	101.6	24.63	12.97	20.83	-10.93	91.4	-2.173	3.48
Val ⁺	-85.33 ^b	-146.42 ^b	45.68 ^h	74.0 ^h	90.9 ^h	21.35 ^h	4.48 ^h	14.58 ^h	-6.12 ^h	83.8 ^h	-4.30 ^h	0.12 ^h
Val ⁺	-88.45 ^y	-146.59 ^y	55.57 ^y	103.5	100.4	27.20	-2.96	-1.29	-3.35	102.5	0.87	0.08
Val ⁻	-72.07 ^y	-138.36 ^y	28.23 ^y	54.8	88.8	20.38	8.07	18.60	-8.00	76.8	-6.27	0.79

states were referenced from a report by Dick et al. (2006) for all of the coded amino acids except for Gly and Met, which were referenced respectively from Kitadai (2014) and LaRowe and Dick (2012). A complete set of $\Delta_f G^\circ$ and $\Delta_f H^\circ$ values for the ionized amino acids has already been calculated by Amend and Helgeson (1997) from data for the corresponding zwitterionic states (Amend and Helgeson 1997) in combination with the standard molal properties of ionization ($\Delta_i G^\circ$ and $\Delta_i H^\circ$) reported by Rodante (1989) for all amino acids except for His, which were referred from Martell and Smith (1982) in accord with

$$\Delta_f G^\circ(\text{ionization state}) = \Delta_f G^\circ(\text{zwitterionic state}) + \Delta_i G^\circ \quad (1)$$

and

$$\Delta_f H^\circ(\text{ionization state}) = \Delta_f H^\circ(\text{zwitterionic state}) + \Delta_i H^\circ \quad (2)$$

Those values, however, cannot accurately represent the temperature dependences of the ionization constants of amino acids reported in the literature (data not shown). Therefore, the values of $\Delta_f G^\circ$ and $\Delta_f H^\circ$ for the ionization states (except for Gly⁺, Gly⁻, and Cys⁻, which were taken from a report by Kitadai (2014) for Gly⁺, Gly⁻, and from one by Dick et al. (2006) for Cys⁻), were revised in the present study using the procedure adopted by Amend and Helgeson (1997) using experimental $\Delta_i G^\circ$ and $\Delta_i H^\circ$ data reported more recently (Ala⁺ and Ala⁻, Ziemer et al. 2006c; Arg⁺, Arg²⁺, His⁺, His²⁺, His⁻, Leu⁺, Leu⁻, Phe⁺, Phe⁻, Trp⁺, Trp⁻, Tyr⁺, Tyr⁻ and Tyr²⁻, Smith and Martell 2004; Arg⁻, Lys⁺, Lys⁻, Lys²⁺, Nagai et al. 2008; Asn⁺, Asn⁻, Kochergina et al. 2011; Asp⁺ and Asp⁻, Glu⁺ and Glu⁻, Ziemer and Woolley 2007c; Asp²⁻ and Glu²⁻, Hamborg et al. 2007; Cys⁺ and Cys²⁻, Goldberg et al. 2002; Gln⁺, Gln⁻, Kochergina et al. 2013; Ile⁺ and Ile⁻, Thr⁺ and Thr⁻, Ziemer and Woolley 2007a; Met⁺ and Met⁻, Ziemer and Woolley 2007b; Pro⁺ and Pro⁻, Sorenson et al. 2003; Ser⁺ and Ser⁻, Ziemer et al. 2006b; Val⁺ and Val⁻; Price et al. 2003b). The values of S° at 25 °C and 1 bar for the ionization states were subsequently calculated from the values of $\Delta_f G^\circ$ and $\Delta_f H^\circ$ presented in Table 1 using values of S° for elements (O₂(g), H₂(g), C(graphite), N₂(g), and S(cr; rhombic)) referred from a report by Cox et al. (1989) (see Eq. (A4)).

Retrieval of the Revised HKF Equations of State Parameters

A complete set of the revised HKF parameters and the standard molal heat capacity (C_p°) and volume (V°) values at 25 °C and 1 bar for the 20 protein amino acids was obtained as follows.

All values for the zwitterionic states and Arg⁺, Arg⁻, Asp⁻, Cys⁻, Glu⁻, His⁺, Lys⁺, Lys⁻, and Tyr⁻ were taken from a report by Dick et al. (2006), whereas those for Gly⁺ and Gly⁻ were taken from a report by Kitadai (2014). The values of c_1 , c_2 and ω for Ala⁺, Ala⁻, Asp⁺, Glu⁺, His⁻, Ile⁺, Ile⁻, Met⁺, Met⁻, Pro⁺, Pro⁻, Ser⁺, Ser⁻, Thr⁺, Thr⁻, Val⁺, and Val⁻ were retrieved by simultaneous regression of experimental C_p° data as a function of temperature (Jardine et al. 2001; Price et al. 2003a,b; Sorenson et al. 2003; Ziemer et al. 2006b,c; Ziemer and Woolley 2007a,b,c) with Eqs. (A13) and (A17). An example of the regression is presented in Fig. 1a as a line on plots of $\Delta C_{p,n}^\circ$ vs. $1/(T-\Theta)^2$ for Ser⁺. The values of $\Delta C_{p,n}^\circ$, the non-solvation contribution to C_p° of Ser⁺, were calculated from Eq. (A17) using experimental C_p° data together with the value of ω presented in Table 1. A value of ω was chosen, which linearized the trend of data points in the regression plots in this figure based on least-squares method. It follows from Eq. (A13) that the intercept and slope of the regression line correspond respectively to c_1 and c_2 . The obtained ω for each amino acid was then combined with experimental V° values provided in the reports noted above to calculate ΔV_n° from Eqs. (A14) and (A18). Regression lines of ΔV_n° as a function of $1/(T-\Theta)$ (e.g. Fig. 1b) have

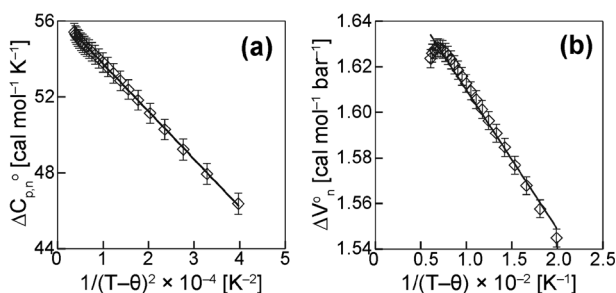


Fig. 1 **a** Nonsolvation contribution to the standard molal heat capacity ($\Delta C_{p,n}^{\circ}$) of Ser^+ as a function of $1/(T-\Theta)^2$. **b** Nonsolvation contribution to the standard molal volume (ΔV_n°) of Ser^+ as a function of $1/(T-\Theta)$. Symbols denote experimental data reported in the literature. Lines present results of regression analysis obtained in this study

the intercept of σ and slope of ξ (Eq. (A14)). Experimental compressibility data as a function of temperature, which are necessary to retrieve values of a_2 and a_4 from Eq. (A8), are not available in the literature for the 17 species listed above. The values of a_2 and a_4 were therefore estimated provisionally from correlations between V° , a_2 and a_4 for cationic and anionic states of amino acids given in a report by Dick et al. (2006) ($a_2 \times 10^{-2} = -1.25 + 0.105 \times V^{\circ}$ and $a_4 \times 10^{-4} = -2.18 - 0.721 a_2 \times 10^{-2}$ for anionic states, and $a_2 \times 10^{-2} = -13.50 + 0.105 \times V^{\circ}$ and $a_4 \times 10^{-4} = -5.48 - 0.721 a_2 \times 10^{-2}$ for cationic states). By combining the obtained σ , ξ , a_2 , and a_4 values using Eqs. (A15) and (A16), the values of a_1 and a_3 were calculated. Table 1 presents the obtained revised HKF parameters, together with the C_p° and V° values at 25 °C and 1 bar calculated from Eqs. (A17) and (A18). These values show close agreement between the predicted and experimental C_p° data as a function of temperature (Fig. 2a–i). The values, however, do not accurately represent the temperature dependences of V° of several amino acids determined experimentally (Fig. 2j–r) (e.g., the predicted value of V° for Ala^+ at 120 °C is $72.1 \text{ cm}^3 \text{ mol}^{-1}$, which is $1.6 \text{ cm}^3 \text{ mol}^{-1}$ lower than that reported by Ziemer et al. (2006c, b, c); $73.7 \text{ cm}^3 \text{ mol}^{-1}$). However, the error in volumetric units ($1.6 \text{ cm}^3 \text{ mol}^{-1}$) corresponds to an energetic error of only $0.04 \text{ cal mol}^{-1} \text{ bar}^{-1}$, which is small compared to the uncertainty associated with C_p° . Consequently, the error in V° only slightly influences the equilibrium calculations for the relevant species. As demonstrated in the next section, a predicted curve for Ala^{\pm} protonation ($\text{Ala}^{\pm} + \text{H}^+ \rightarrow \text{Ala}^+$) calculated using the data and parameters presented in Table 1 are closely consistent with the corresponding experimental measurements in a broad temperature range (0–250 °C; Fig. 5a). Deviation of calculated V° values from experimental ones (Fig. 2j–r) has also been observed for other amino acids, particularly at higher temperatures (Kitadai 2014; Dick et al. 2006).

Sufficient experimental calorimetric and volumetric data as a function of temperature are not available in the literature for other ionization states of amino acids to generate a regression for retrieval of their revised HKF parameters. Instead, these parameters were calculated from correlation algorithms using values obtained using the procedures explained above. Figure 3 presents correlations of C_p° , V° , σ , and c_l of the zwitterionic state and the cationic state (or the zwitterionic state and the anionic state) of neutral amino acids (Ala, Gly, Ile, Met, Ser, Thr, and Val). The values for Pro were not included in this figure because Pro has an imino group instead of the amino group. Each correlation shows good linear relations particularly for C_p° and V° . The correlation lines depicted in each figure were therefore used to estimate the values of C_p° , V° , σ , and c_l for Asn^+ , Asn^- , Gln^+ , Gln^- , Leu^+ , Leu^- , Phe^+ , Phe^- , Trp^+ and Trp^- from

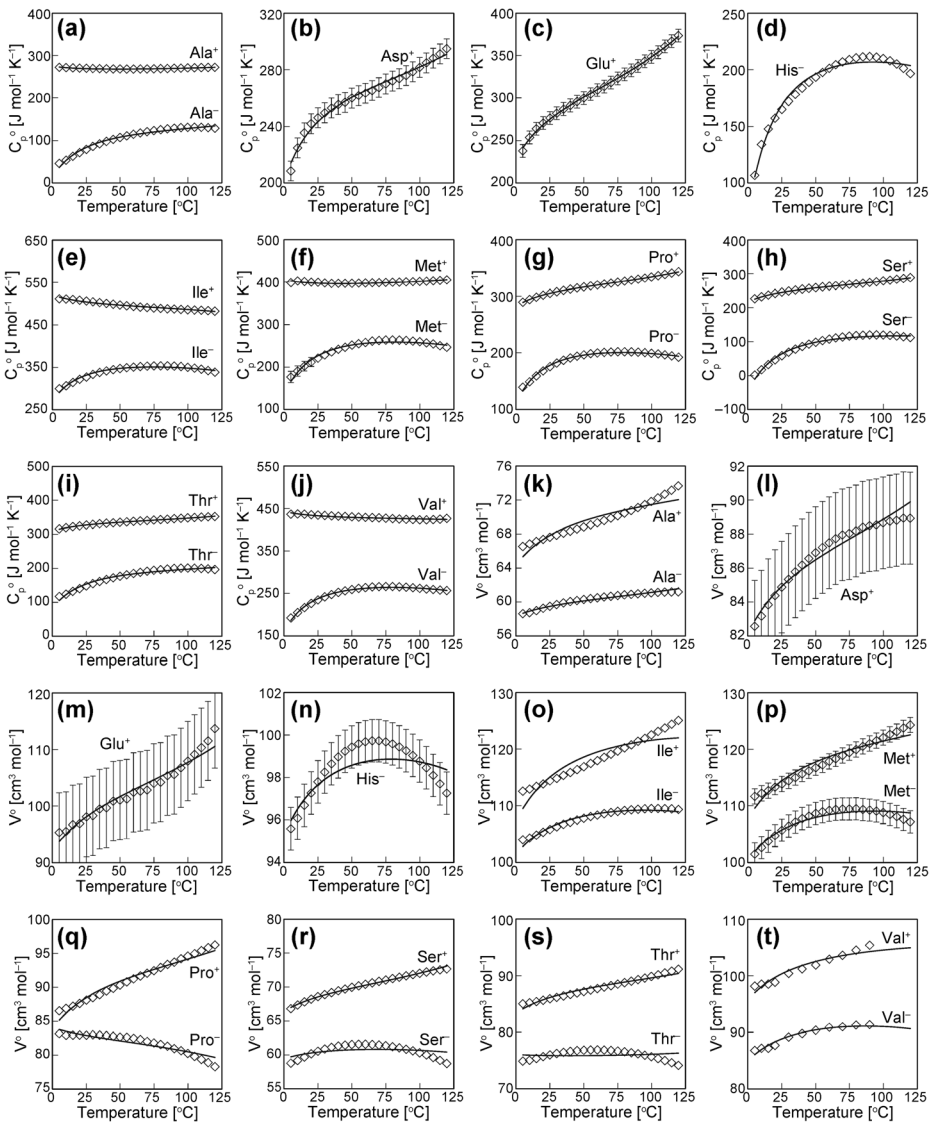


Fig. 2 Standard molal heat capacity (C_p^o , **(a)–(i)**) and volume (V^o , **(j)–(r)**) of ionized amino acids as a function of temperature. Curves were calculated using the revised HKF equations of state together with thermodynamic data and HKF parameters presented in Table 1. Symbols denote experimental data reported in the literature: Ala (Ziemer et al. 2006c), Asp and Glu (Ziemer and Woolley 2007c), His (Jardine et al. 2001; Price et al. 2003a), Ile and Thr (Ziemer and Woolley 2007a), Met (Ziemer and Woolley 2007b), Pro (Sorenson et al. 2003), Ser (Ziemer et al. 2006b), and Val (Price et al. 2003b). No error bar is shown in this figure when the reported uncertainty associated with the experimental data is less than the symbol size

the values for their zwitterionic states presented in Table 1 (values of σ for their zwitterionic states were calculated from Eq. (A15) using the values of a_1 and a_2 presented in Table 1).

The cationic states of neutral amino acids are formed from the corresponding zwitterionic states by the protonation of the α -carboxylic group ($-\text{COO}^- + \text{H}^+ \rightarrow -\text{COOH}$). For basic amino acids (Arg, His, and Lys), the protonation of the α -carboxylic group occurs when their

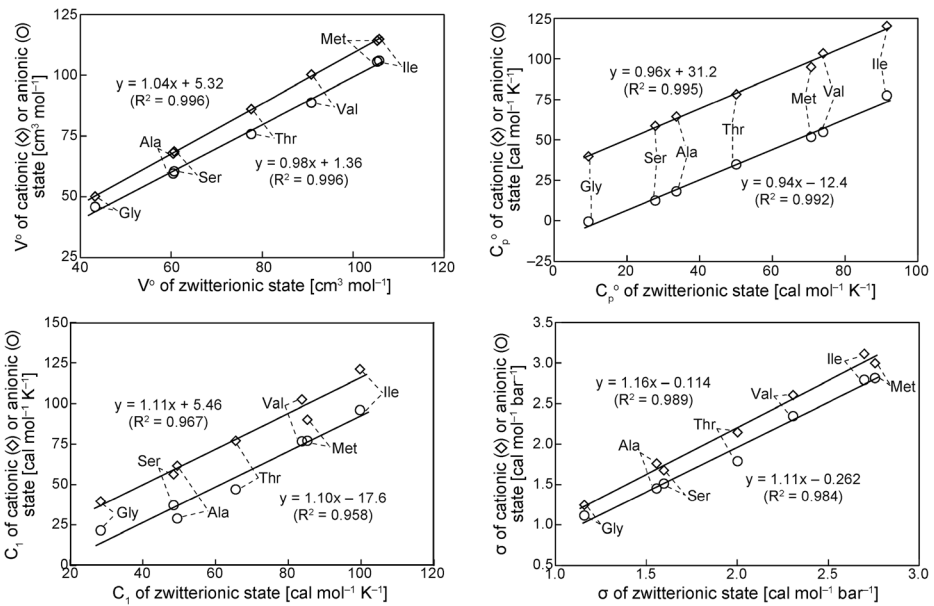


Fig. 3 Correlations of C_p° , V° , σ , and c_I of the zwitterionic state and the cationic state (or the zwitterionic state and the anionic state) of neutral amino acids (Ala, Gly, Ile, Met, Ser, Thr, and Val)

speciations change from a cationic to a di-cationic state. The zwitterionic vs. cationic correlations depicted in Fig. 3 were therefore used to estimate the values of C_p° , V° , σ , and c_I for Arg^{2+} , His^{2+} and Lys^{2+} from those for Arg^+ , His^+ and Lys^+ presented in Table 1. The correlations were also used to estimate the values for Cys^+ and Tyr^+ from those for Cys^\pm and Tyr^\pm presented in Table 1 because these amino acids protonate their α -carboxylic group in the zwitterionic to cationic transformation.

Similarly, speciation change of neutral amino acids from zwitterionic to anionic state involves deprotonation of the α -amino group ($-\text{NH}_3^+ \rightarrow -\text{NH}_2 + \text{H}^+$). The deprotonation is observed in acidic amino acids (e.g. Asp) when their speciation changes from an anionic to a di-anionic state. The zwitterionic vs. anionic correlations presented in Fig. 3 were therefore used to estimate the values for Asp^{2-} , Cys^{2-} and Glu^{2-} from those for Asp^- , Cys^- , and Glu^- presented in Table 1.

The methodologies are inapplicable to estimation of the values for Tyr^{2-} because Tyr^{2-} is formed from Tyr^- by side chain hydroxyl group ($-\text{OH} \rightarrow -\text{O}^- + \text{H}^+$) deprotonation. The values of C_p° , V° , σ , and c_I for Tyr^{2-} were therefore calculated provisionally on the assumption that the side chain hydroxyl group of Tyr ($\text{Tyr}^- \rightarrow \text{Tyr}^{2-} + \text{H}^+$) deprotonation causes the same changes in the values of C_p° , V° , σ , and c_I as those generated by the side chain carboxyl group of Glu ($\text{Glu}^\pm \rightarrow \text{Glu}^- + \text{H}^+$) deprotonation. The calculations can be represented as

$$\Xi_{\text{Tyr}^{2-}} = \Xi_{\text{Tyr}^-} (\Xi_{\text{Glu}^\pm} - \Xi_{\text{Glu}^-}) \quad (3)$$

Therein, Ξ stand for C_p° , V° , σ , and c_I of the respective species.

Provisional estimates of ω for the cationic (Asn^+ , Gln^+ , Leu^+ , Phe^+ , Trp^+ , Cys^+ and Tyr^+) and anionic (Asn^- , Gln^- , Leu^- , Phe^- , and Trp^-) amino acids were calculated using the correlations between ω and the standard molal entropy of hydration ($\Delta S_{\text{hyd}}^\circ$) reported by Dick et al. (2006). Also, the values of $\Delta S_{\text{hyd}}^\circ$ for the amino acids were referred from that

report. The correlations between ω and ΔS_{hyd}^o of alkali-group and fluoride-group metal ions (Dick et al. 2006) were used, respectively, to estimate the values of ω for the cationic and anionic amino acids. Similarly, the values of ω for the di-cationic (Arg^{2+} , His^{2+} and Lys^{2+}) and di-anionic (Asp^{2-} , Cys^{2-} and Glu^{2-} and Tyr^{2-}) amino acids were calculated using the correlations between ω and ΔS_{hyd}^o for the alkaline earth metal ions and various divalent anions presented in Fig. 4. The values of ΔS_{hyd}^o shown in this figure were referred from a report by Marcus (1994). Those of ω were referred from another report by Shock et al. (1997), except for $\text{C}_2\text{O}_4^{2-}$ (Shock 1995).

The values of c_2 for the amino acids were then calculated from Eq. (A17) using the values of C_P^o , c_1 , and ω presented in Table 1.

The values of a_1 , a_2 , a_3 , and a_4 for the cationic (Asn^+ , Gln^+ , Leu^+ , Phe^+ , Trp^+ , Cys^+ and Tyr^+) and anionic (Asn^- , Gln^- , Leu^- , Phe^- , and Trp^-) amino acids were estimated as follows. First, the values of a_2 and a_4 were calculated using correlations between V^o , a_2 and a_4 reported by Dick et al. (2006). The values of a_2 were then used, together with the values of σ estimated using the foregoing procedures, to calculate the values of a_1 from Eq. (A15). The values of a_3 were calculated from Eqs. (A15), (A16), and (A18) using the values of a_1 , a_2 , a_4 , and V^o presented in Table 1.

No correlation equations or high-temperature calorimetric and volumetric data are available in the literature for the values of a_1 , a_2 , a_3 , and a_4 for di-cationic (Arg^{2+} , His^{2+} and Lys^{2+}) and di-anionic (Asp^{2-} , Cys^{2-} and Glu^{2-} and Tyr^{2-}) amino acids. Dick et al. (2006) demonstrated that the slopes of the correlations between V^o , a_2 , and a_4 for cationic, anionic and zwitterionic amino acids are independent of charge, although the intercepts are charge-dependent. Therefore, the slopes of the correlations for di-cationic and di-anionic amino acids were assumed to be roughly equal to those for the other ionization states of amino acids. The intercepts for di-cationic amino acids were estimated on the assumption that the intercepts differ from those for cationic amino acids by the same values as the differences between the intercepts for cationic amino acids and zwitterionic amino acids. The intercepts for di-anionic amino acids were calculated similarly. The estimated correlation equations are written as

$$a_2 \times 10^{-2} = -22.20 + 0.105 \times V^o \quad (4)$$

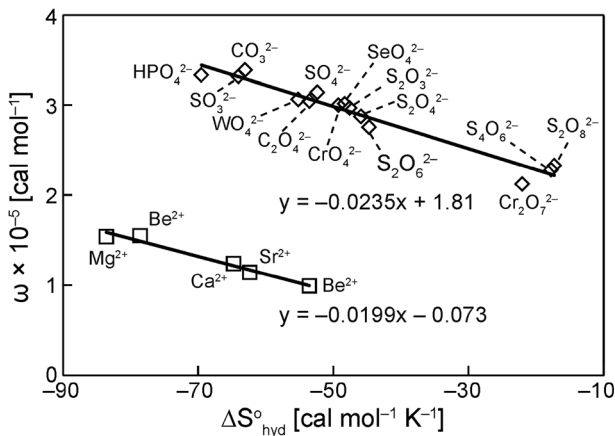


Fig. 4 Correlations between ω and ΔS_{hyd}^o at 25 °C and 1 bar for alkaline earth metal ions (\square) and various divalent anions (\diamond). Values of ΔS_{hyd}^o presented in this figure were referred from a report by Marcus (1994). Those of ω were referred from Shock et al. (1997), except for $\text{C}_2\text{O}_4^{2-}$, which was referred from Shock (1995)

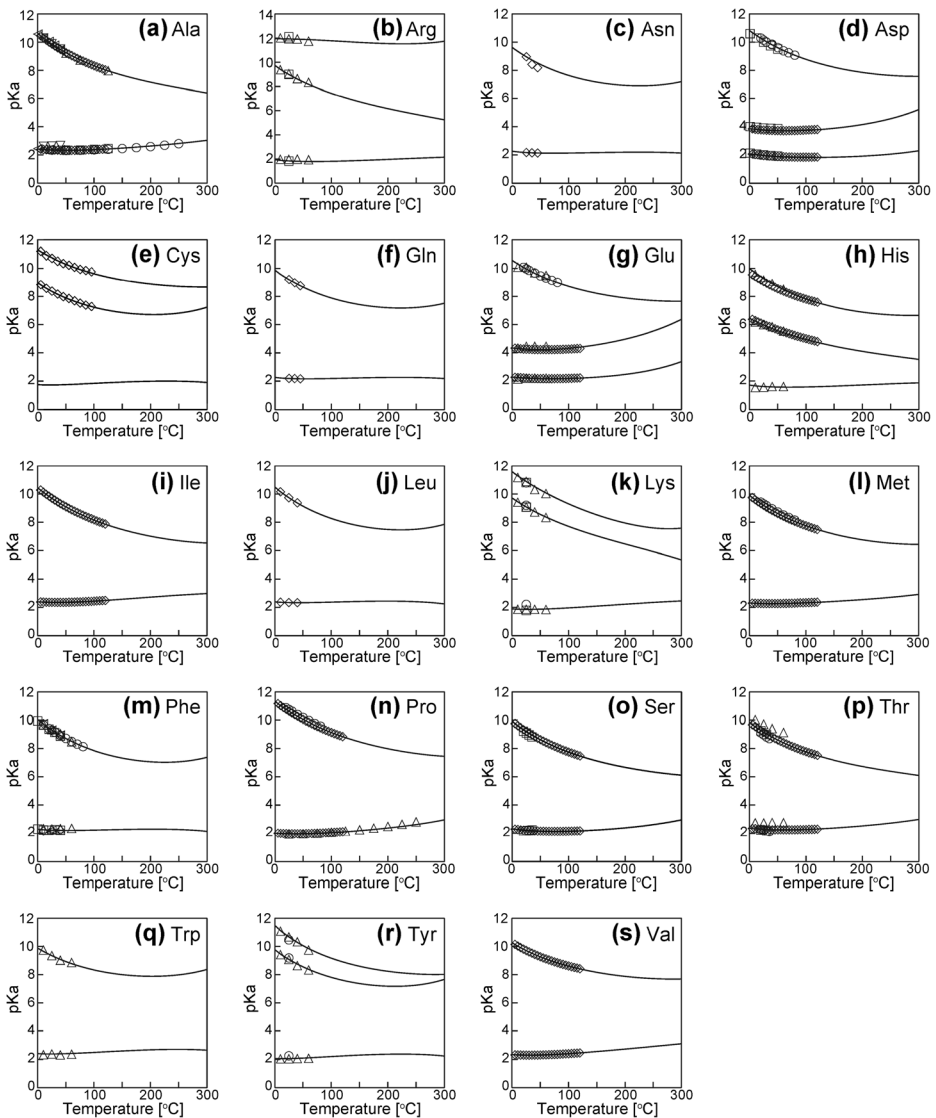


Fig. 5 First, second, and third dissociation constants of the 19 protein amino acids. *Curves* were calculated with the revised HKF equations of state together with the thermodynamic data and the revised HKF parameters presented in Table 1. *Symbols* denote experimental data reported in the literature: Ala (\triangleleft , Izatt et al. 1961; ∇ , Anderson et al. 1967; Δ , Gillespie et al. 1995; \square , Wang et al. 1996; \circ , Clarke et al. 2005; \diamond , Ziemer et al. 2006c), Arg (\square , Smith and Martell 2004; Δ , Nagai et al. 2008), Asn (\diamond , Kochergina et al. 2011), Asp (\square , Smith and Smith 1942; \diamond , Ziemer and Woolley 2007c; \diamond , Hamborg et al. 2007), Cys (\diamond , Coates et al. 1969), Gln (\diamond , Kochergina et al. 2013), Glu (\diamond , Ziemer and Woolley 2007c; \circ , Hamborg et al. 2007; Δ , Nagai et al. 2008), His (\diamond , Price et al. 2003a; Δ , Nagai et al. 2008), Ile (Δ , Ziemer and Woolley 2007a), Leu (\diamond , Smith and Martell 2004), Lys (\square , Smith and Martell 2004; \circ , Humblot et al. 2006; Δ , Nagai et al. 2008), Met (\diamond , Ziemer and Woolley 2007b; \circ , Hamborg et al. 2007), Phe (\square , Izatt et al. 1961; \diamond , Anderson et al. 1966; \triangleleft , Smith and Martell 2004; \circ , Hamborg et al. 2007; Δ , Nagai et al. 2008), Pro (\diamond , Sorenson et al. 2003; Δ , Clarke et al. 2005; \circ , Hamborg et al. 2007), Ser (\square , Gergely et al. 1972; \diamond , Ziemer et al. 2006b), Thr (\square , Izatt et al. 1964; \circ , Gergely et al. 1972; \diamond , Ziemer and Woolley 2007a; Δ , Nagai et al. 2008), Trp (Δ , Nagai et al. 2008), Tyr (\circ , Smith and Martell 2004; Δ , Nagai et al. 2008), and Val (\diamond , Price et al. 2003b)

and

$$a_4 \times 10^{-4} = -8.18 - 0.721a_2 \times 10^{-2} \quad (5)$$

for di-cationic states, and

$$a_2 \times 10^{-2} = 2.30 + 0.105 \times V^o \quad (6)$$

and

$$a_4 \times 10^{-4} = -1.58 - 0.721a_2 \times 10^{-2} \quad (7)$$

for di-anionic states. Values of a_1 and a_3 were then calculated using a_2 , a_4 , σ , and V^o presented in Table 1 from Eqs. (A15), (A16), and (A18).

Based on group additivity algorithms developed by Amend and Helgeson (1997, 2000) and Dick et al. (2006), thermodynamic properties of an amino acid are separable into two contributions as shown below.

$$\Xi_{AA} = \Xi_{[AABB]} + \Xi_{[SC]} \quad (8)$$

Therein, Ξ_{AA} , $\Xi_{[AABB]}$, and $\Xi_{[SC]}$ respectively stand for any thermodynamic data or revised HKF parameters for the amino acid, amino acid backbone, and side-chain group. Because a complete set of the data and parameters for the 20 protein amino acids was obtained using the procedure described above, these were then used to calculate the corresponding values of [AABB] and [sc]. The calculation procedure and retrieved values are presented in Appendix B.

Energetics of Amino Acid Synthesis Under Alkaline Hydrothermal Systems

A complete set of the standard molal thermodynamic data is presented in Table 1 along with the revised HKF parameters for the 20 protein amino acids. This set enables, for the first time, prediction of the thermodynamic behavior of amino acids over broad ranges of temperature and pH. For instance, Fig. 5 shows the dissociation constants (pK_a) of 19 amino acids (curves), together with the corresponding experimental measurements reported in the literature (symbols), for temperatures of 0–300 °C (the pK_a values of Gly are not shown in this figure, but are presented in another report; Kitadai 2014). The curves were calculated using the following equation.

$$\Delta_r G^o = -RT \ln K \quad (9)$$

Therein, T and R stand for the temperature in units Kelvin and the gas constant (8.31447 J mol⁻¹ K⁻¹); $\Delta_r G^o$ denotes the standard Gibbs energy of reaction. The value of $\Delta_r G^o$ was calculated by combining the standard Gibbs energies of formation (ΔG^o) of the individual compounds involved in the reaction.

$$\Delta_r G^o = \sum \Delta G^o_{products} - \sum \Delta G^o_{reactants} \quad (10)$$

The ΔG^o of amino acids at any temperature and pressure was calculated from Eq. (A19) using the data and parameters presented in Table 1. Pressure was set to 1 bar at <100 °C, with saturated water vapor pressure (P_{sat}) at ≥ 100 °C. It is apparent in Fig. 5 that the predicted curves show close agreement with the experimental measurements for each reaction at all temperatures. The agreement supports the validity of the dataset presented in Table 1. It is noteworthy that the experimental measurements at temperatures higher than 150 °C are not available in the literature for most of the amino acids, likely because the amino acids themselves decompose

rapidly under such conditions. Thermodynamic predictions depicted in Fig. 5 thus provide useful information for the ionization states of amino acids in experimentally inaccessible region.

To evaluate whether or not an alkaline hydrothermal system is favorable for the abiotic synthesis of amino acids, which may be a necessary step for the chemical evolution of life (e.g. Rode 1999), Gibbs energies necessary to synthesize amino acids from inorganic precursors in such systems were calculated. Several researchers have estimated the composition of fluids in primitive hydrothermal systems (e.g., Macleod et al. 1994; Amend and McCollom 2009). Recently, Shibuya et al. (2010) reported, based on thermodynamic calculations, that deep-sea hydrothermal systems in the Hadean and early Archean periods were dominated by highly alkaline (pH >10), high-temperature (approx. 350 °C) hydrothermal activity even at the spreading zone because of a high concentration of ΣCO_2 in the early ocean (>0.2 mol/kg). High dissolved ΣCO_2 keeps the activity of Ca^{2+} very low owing to the precipitation of calcite ($\text{Ca}^{2+} + \text{CO}_3^{2-} \rightarrow \text{CaCO}_3$), which then increases pH through reactions between plagioclase and epidote ($2\text{Ca}_2\text{Al}_3\text{Si}_3\text{O}_{12}(\text{OH}) + 2\text{H}^+ \leftrightarrow 3\text{CaAl}_2\text{Si}_2\text{O}_8 + \text{Ca}^{2+} + 2\text{H}_2\text{O}$) (Shibuya et al. 2010). That prediction was later supported by results of a heating experiment using basalt and CO_2 -rich seawater at 250 and 350 °C (Shibuya et al. 2013). In the present calculation, the CO_2 concentration in the simulated Hadean seawater was set to 200 mmol/kg (the atmospheric CO_2 pressure equilibrated with the simulated seawater is about 5 bar; Helgeson et al. 1978; Shock et al. 1989). The temperature and pH of the hydrothermal fluid were set to 350 °C and 10.0, respectively (Table 2). The pH of the Hadean seawater was assumed to be 5.0 (Russell 2003; Russell et al. 2010). The temperature of the Hadean ocean is still under debate, ranging from 90 °C (Russell and Hall 1997) to less than 0 °C (Bada et al. 1994; Bada 2004) depending on interpretation of geological records. I choose a conservative temperature of 25 °C because of the absence of consensus. Other dissolved species than CO_2 , and their concentrations in the ocean and in the hydrothermal fluid were taken from an estimation by Amend and McCollom (2009) except for the Cl^- concentration, which was varied to adjust the pH of the two end-members to desired values (pH10.0 for the hydrothermal fluid and pH5.0 for the Hadean

Table 2 Compositions of end-member fluids used in the mixing calculations (all concentrations, millimolal)

	Seawater	Hydrothermal fluid
T [°C]	25	350
pH	5.0	10.0
$\text{H}_2(\text{aq})$	0.00054	16
ΣCO_2	200	0.01
$\text{O}_2(\text{aq})$	10^{-9}	0
Na	464	607
Cl	539	516
Ca	14.2	20
Mg	31.1	0.001
Fe	0.12	0
K	0.1	10
CH_4	0	2.0
$\Sigma\text{H}_2\text{S}$	0.0002	0.1
SO_4^{2-}	0.1	0
$\text{SiO}_2(\text{aq})$	0.11	0.005
NH_3	10^{-5}	10^{-5}

seawater). Amend and McCollom (2009) defined the fluid composition based on the composition of the Lost City vent fluids. Their estimation therefore is directly applicable in this study to simulate amino acid synthesis under Hadean alkaline hydrothermal systems. The composition of the Hadean seawater allows complete dissolution of minerals including calcite (CaCO_3), magnesite (MgCO_3), siderite (FeCO_3), brucite ($\text{Mg}(\text{OH})_2$), pyrrhotite (FeS), and pyrite (FeS_2).

The two solutions were then mixed to simulate mixing of the hydrothermal fluid with seawater near such hydrothermal systems. The model starts with 100 % seawater at 25 °C with subsequent gradual increases of the percentage of vent fluid at 350 °C. The composition and chemical speciation of the mixed fluid were recalculated continuously after each step. The temperature of the mixed solution was assumed to change in proportion to the mixing ratio of the two end-member fluids. Pressure was set to 250 bar. The effect of pressure on the ΔG° of amino acids is small compared with that of temperature (Shock 1992). Thus, calculation results presented below do not significantly change if deeper (500 bar; ~5000 m) or shallower (10 bar; ~100 m) ocean vents are considered. All redox reactions were presumed to be inhibited kinetically on the timescales of mixing (Amend and McCollom 2009). It has been shown that redox reactions among single carbon compounds other than CH_4 (CO_2 , CO , HCOOH , CH_3OH) reach their equilibria rapidly at high temperature condition (>225 °C) (McCollom and Seewald 2003; Seewald et al. 2006). At equilibrium, however, thermodynamic drives for the abiotic synthesis of amino acids from these compounds are the same. To simplify data interpretation, possible existences of the reduced forms of CO_2 were not considered in the fluid mixing calculation. Minerals were allowed to precipitate during the mixing, except for graphite and dolomite, which were presumed to be kinetically inhibited (Amend and McCollom 2009). All calculations were performed using the Visual MINTEQ version 2.61 computer program. The thermodynamic datasets needed for this calculation were generated from Eqs. (A19), (9), and (10) using thermodynamic data and the revised HKF parameters for minerals (Helgeson et al. 1978), aqueous species (Shock et al. 1989, 1997) and complexes (Sverjensky et al. 1997; McCollom and Shock 1997). The ΔG° of H_2O at any temperature and pressure was calculated using polynomial equations reported by Helgeson and Kirkham (1974). Activity coefficients for aqueous species were calculated using the extended Debye–Huckel equation (Helgeson et al. 1981).

Figure 6 presents changes in the activities of $\text{CO}_{2,\text{Tot}}$ ($= a_{\text{CO}_2} + a_{\text{HCO}_3^-} + a_{\text{CO}_3^{2-}}$), $\text{NH}_{3,\text{Tot}}$ ($= a_{\text{NH}_3} + a_{\text{NH}_4^+}$), $\text{H}_2\text{S}_{\text{Tot}}$ ($= a_{\text{H}_2\text{S}} + a_{\text{HS}^-}$; S^{2-} was not considered because the dissociation constant of HS^- is very small ($K=10^{-18.51}$ at 20 °C; Schoonen and Barnes 1988), implying that S^{2-} is never a dominant aqueous species), and H_2 and pH during mixing. The activities of $\text{H}_2\text{S}_{\text{Tot}}$ and H_2 showed steep increases at the initial stage of the mixing in the logarithmic scale. They then increased gradually with the mixing ratio of vent fluid. A reverse trend was observed for the activity of $\text{CO}_{2,\text{Tot}}$. pH showed a sigmoid-type increase, with the center at about 225 °C. This result is mainly owing to the buffering effect of CO_2 . As can be seen in Fig. 7, a speciation change of CO_2 to HCO_3^- is calculated with the center at about 225 °C. A similar changing pH trend was reported for a mixing calculation by Amend and McCollom (2009). However, their reported curve is steeper than that observed in this study because their simulated concentration of CO_2 in seawater ($22.7 \text{ mmol kg}^{-1}$) is about one order of magnitude smaller than that assumed in this study (200 mmol kg^{-1}). Lower CO_2 concentrations have a smaller buffering effect on pH, making pH change more sharply.

The Gibbs energy of reaction ($\Delta_r G$) of amino acid synthesis is calculable using the following equation as

$$\Delta_r G = \Delta_r G^\circ + RT \ln Q_r \quad (11)$$

in which Q_r stands for the activity product given as shown below.

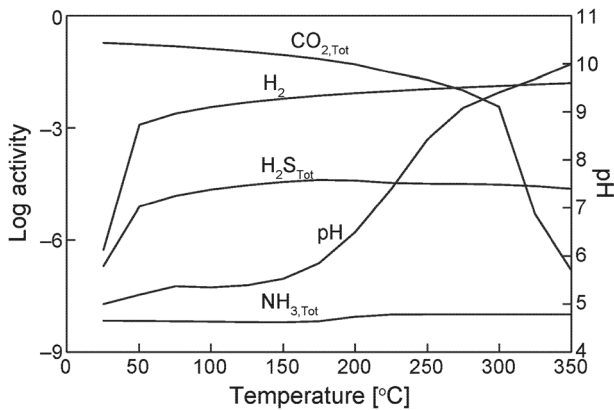


Fig. 6 Calculated activities of $\text{CO}_{2,\text{Tot}}$ ($= a_{\text{CO}_2} + a_{\text{HCO}_3^-} + a_{\text{CO}_3^{2-}}$), $\text{NH}_{3,\text{Tot}}$ ($= a_{\text{NH}_3} + a_{\text{NH}_4^+}$), $\text{H}_2\text{S}_{\text{Tot}}$ ($= a_{\text{H}_2\text{S}} + a_{\text{HS}^-}$) and H_2 and pH resulting from mixing of seawater with alkaline hydrothermal fluid presented in Table 2

$$Q_r = \prod_i a_i^{\nu_{i,r}} \quad (12)$$

Therein, $\nu_{i,r}$ stands for the stoichiometric reaction coefficient of the i th species in the reaction, which is positive for products and negative for reactants. As inorganic precursors, this study selected CO_2 , NH_3 , H_2S , and H_2 respectively as sources of carbon, nitrogen, sulfur, and hydrogen. CH_4 was not used instead of CO_2 because CH_4 formation from CO_2 ($\text{CO}_2 + 4\text{H}_2 \rightarrow \text{CH}_4 + 2\text{H}_2\text{O}$) is a strong thermodynamically favorable reaction (e.g., $\Delta_r G^\circ = -195 \text{ kJ mol}^{-1}$ at 25°C and 250 bar (Helgeson and Kirkham 1974; Shock et al. 1989; Shock and Helgeson 1990)). Consequently, syntheses of amino acids from CH_4 require much larger amounts of extra energy than those from CO_2 . Nitrogen oxides (NO_2^- , NO_3^- , etc.) and sulfur oxides (SO_3^{2-} , SO_4^{2-} , etc.) might be regarded as alternate sources of nitrogen and sulfur. However, direct formation of amino acids from these compounds in aqueous solution has not been reported in the relevant literature. The combination of CO_2 , NH_3 , H_2S , and H_2 has also been used in several thermodynamic calculations for abiotic syntheses of biomolecules under hydrothermal systems

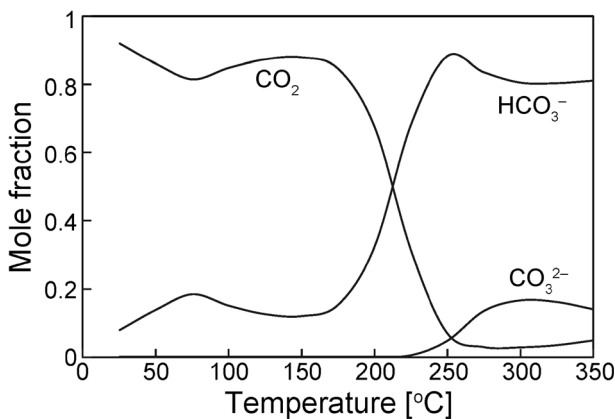


Fig. 7 Mole fractions of CO_2 , HCO_3^- , and CO_3^{2-} as a function of temperature at 250 bar during mixing of seawater and alkaline hydrothermal fluid presented in Table 2

(Amend and Shock 1998; McCollom and Amend 2005; Amend and McCollom 2009; Shock and Canovas 2010). The choice of these compounds supports direct comparisons of the results obtained in the present study with those of the reported studies. The synthesis equations of amino acids from the compounds have been presented in earlier reports (e.g., Table 1 in Amend and Shock 1998). For that reason, they are not shown in this manuscript. The equations were used together with the fluid compositions determined with the mixing model (Fig. 6) to calculate the $\Delta_r G$ necessary to synthesize amino acids at each mixing step from Eq. (11). The activity of each amino acid was set to 10^{-6} (Shock and Canovas 2010). The value (10^{-6}) was selected arbitrary because the concentrations of amino acids in the Hadean ocean and hydrothermal fluids are not known. Consequently, negative $\Delta_r G$ means that the aqueous environment can synthesize amino acids with activities of more than 10^{-6} , although positive values do not.

Figure 8 shows the $\Delta_r G$ of synthesis of the 20 protein amino acids as a function of temperature. The values of $\Delta_r G$ decreased drastically at temperatures from 25 to 50 °C. Then they increased gradually at higher temperatures for all amino acids. The former declines (25 → 50 °C) are attributable to the rapid increases of the activities of H_2 and H_2S_{Tot} in the same temperature range (Fig. 6). The subsequent increases of $\Delta_r G$, however, cannot be explained clearly from the activity changes of inorganic precursors because the activity of H_2 continues to increase, whereas that of $CO_{2,Tot}$ decreases (Fig. 6). The activity of $NH_{3,Tot}$ also increases slightly at temperatures of around 200 °C (Fig. 6) because of the speciation change from NH_4^+ to NH_3 . To understand the observed changing trends of the $\Delta_r G$, the contributions from the $\Delta_r G^\circ$ -term as well as the compositional variation expressed in the Q_r -term must be considered.

Figure 9 presents the standard Gibbs energies of reaction ($\Delta_r G_{pH}^\circ$) of the amino acid synthesis as a function of temperature and pH, as calculated from Eq. (11) setting the activities of all species to one, except for H^+ . Only the contribution from the activity of H^+ on the Gibbs energies was considered in order to evaluate the pH dependences (the procedure for calculating $\Delta_r G_{pH}^\circ$ is described in Appendix C). The values of $\Delta_r G_{pH}^\circ$ at neutral pH are consistent with the

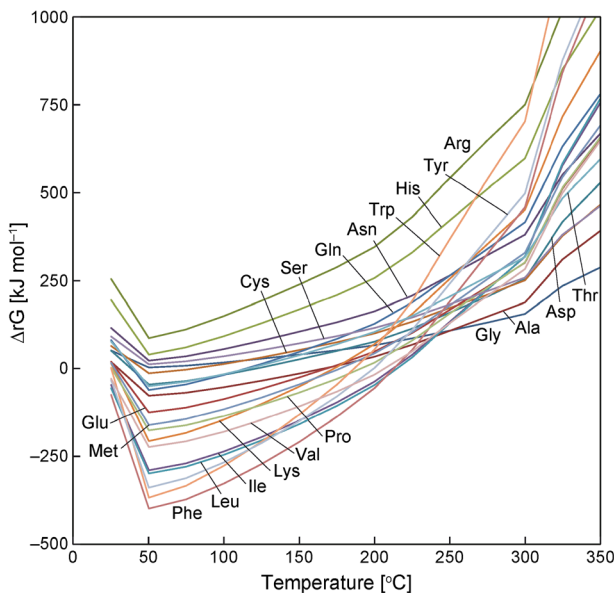


Fig. 8 Calculated $\Delta_r G$ of synthesis of the 20 protein amino acids as a function of temperature at 250 bar during mixing of seawater and alkaline hydrothermal fluid presented in Table 2

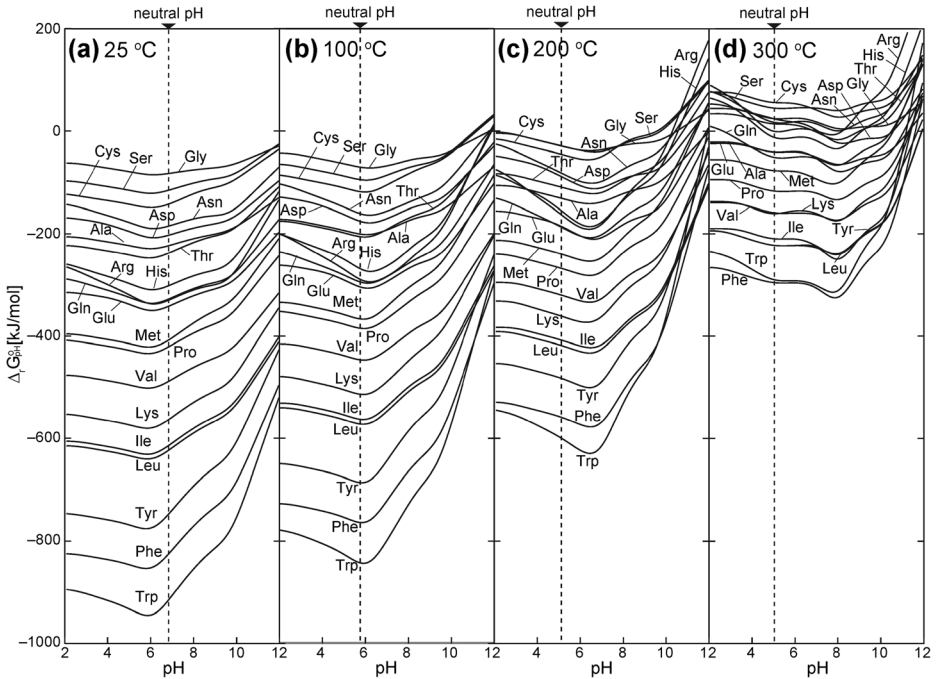


Fig. 9 Standard Gibbs energies of reaction of the amino acid synthesis as a function of temperature and pH ($\Delta_r G_{pH}^\circ$), which was calculated from Eq. (11) setting the activities of all species to one except for H^+ (see the text)

reported counterparts (Amend and Shock 1998; McCollom and Amend 2005; Amend and McCollom 2009) except for Gly and Met, of which the thermodynamic data for their zwitterionic states were updated in this study. At 25 °C, all amino acids showed minimum $\Delta_r G_{pH}^\circ$ at pH of about 6 (Fig. 9). The values increased greatly with increasing pH, particularly at $pH > 10$. At $pH = 11.0$, for instance, the $\Delta_r G_{pH}^\circ$ values are an average of 134 kJ mol^{-1} higher than those at $pH = 6.0$. The energetic gap corresponds to the difference in the equilibrium constant (K) of 3.0×10^{23} (calculated from Eq. (9)). That tremendous value reflects that the energetics of amino acid synthesis have strong pH dependence. At higher temperatures, the positions of the minimum $\Delta_r G_{pH}^\circ$ shifted slightly toward alkaline pH. At 200 °C, the minimum $\Delta_r G_{pH}^\circ$ locates at pH of about 6.5, where the values are an average of 15 kJ mol^{-1} lower than those at neutral pH ($pH = 5.2$ at 200 °C). The superiority, however, is small compared with the subsequent increases of the $\Delta_r G_{pH}^\circ$ at higher pH (Fig. 9). That superiority is also obscured by the greater increase of the $\Delta_r G_{pH}^\circ$ with temperature (Fig. 9). Consequently, amino acid syntheses under higher temperature and alkaline pH are thermodynamically unfavorable compared with those at lower temperature and neutral pH.

The temperature and pH dependences of $\Delta_r G_{pH}^\circ$ (Fig. 9) are a major cause of the gradual increase of the $\Delta_r G$ observed in the mixing calculation at temperatures higher than 50 °C (Fig. 8). Both the increases of temperature and pH (Fig. 6) shift $\Delta_r G$ toward higher values (Fig. 9). Further steep increases of $\Delta_r G$ at > 300 °C (Fig. 8) are attributable to the sharp decline of the activity of CO_2 (Fig. 6). It is noteworthy, however, that the $\Delta_r G$ in the mixing fluid is lower than that in 100 % seawater in a wide temperature range (Fig. 8). The values of $\Delta_r G$ at 50 °C are mostly negative, indicating that many amino acids can be formed at concentrations that are higher than the micro-molar level if the equilibrium can be attained. Such energetic

favorability is a consequence of the mixing between the CO₂-rich seawater and the H₂-rich hydrothermal fluid. A similar changing trend of Δ_rG with a local minimum at about 50 °C was also observed in a mixing calculation by (Amend and McCollom 2009) assuming a lower concentration of CO₂ in seawater (22.7 mmol kg⁻¹) and lower temperature of hydrothermal fluid (140 °C). The H₂ concentration in deep-sea hydrothermal systems in the Hadean period was expected to be much higher than the present level because of the abundant presence of ultramafic rocks called komatiites under the seafloor (Takai et al. 2006; McCollom and Seewald 2013). Unlike basalt, a major constituent of the present oceanic crust, komatiites can produce H₂ effectively through serpentinization because of their low silica content (McCollom and Seewald 2007, 2013). Hadean alkaline hydrothermal systems can therefore be regarded as having good potential for the abiotic synthesis of amino acids assuming kinetic pathways for their synthesis exist, which is not in most cases obviously true. Acidic hydrothermal systems may also be considered as a favorable environment if sufficiently high concentrations of reducing components (H₂, NH₃, H₂S) were provided. However, such systems cannot provide the best pH condition for the amino acid synthesis (neutral; pH~6 at 25 °C) through mixing with the slightly acidic seawater (pH~5). Similarly, if the Hadean seawater was hotter than the assumption made in this study (e.g., 70 °C vs. 25 °C), mixing the seawater with fluids in alkaline hydrothermal systems cannot decrease the temperature sufficiently and consequently, the energetic costs for the synthesis reactions increase. Consequently, hot, alkaline hydrothermal systems beneath cool, slightly acidic Hadean ocean are an energetically excellent setting among possible vent–Ocean combinations. An important strength of the present calculation is that the speciation changes of amino acids as well as inorganic precursors are regarded as functions of temperature and pH. If further geochemical knowledge related to the primitive hydrothermal systems were obtained, more accurate evaluation of the potential for amino acid synthesis would be possible using the same methodology as that adopted in this study.

Early life may have required not only amino acids, but also peptides. It has been shown that the thermodynamic stability of peptides relative to hydrolysis increases with temperature, and that it exhibits a maximum at moderately alkaline pH (e.g., pH of approx. 9.5 at 25 °C) (Shock 1992; Kitadai 2014). If amino acids are present in hydrothermal systems, higher concentrations of peptides can be produced at a higher mixing ratio of hydrothermal fluid. As a test to examine that possibility, the activity of glycylglycine (GlyGly) equilibrated with Gly (activity = 0.001) was calculated assuming the temperature and pH conditions depicted in Fig. 6 using the thermodynamic data and the HKF parameters reported by Kitadai (2014). Results (Fig. 10) show that the activity of GlyGly reaches its maximum level at a temperature of about 225 °C. The optimum temperature is much higher than those for amino acid synthesis (which peak near 50 °C; Fig. 7). Russell and co-workers have proposed that life arose within compartments in FeS (and NiS) precipitates at an alkaline hydrothermal mound, where cool (≤ 20 °C), slightly acidic CO₂-rich Hadean Ocean water (pH 5–6) met hot, reduced alkaline solution rich in H₂, H₂S, and NH₃ (pH 9–11) (Russell 2003; Russell and Martin 2004; Russell et al. 2010). At the vent–ocean interface, ocean water permeates into the vent structure across the precipitated FeS-bearing walls. Inhibition of flow, partial containment and catalytic surfaces provided by the (Fe,Ni)S compartments could potentially produce a highly reactive chemical environment. If amino acids are synthesized in the initial stage of the permeation with the aid of the catalytic activity of (Fe,Ni)S (Huber and Wachtershauser 2006), then subsequent increases of temperature and pH caused by fluid mixing might facilitate polymerization of amino acids. (Fe,Ni)S can also catalyze amino

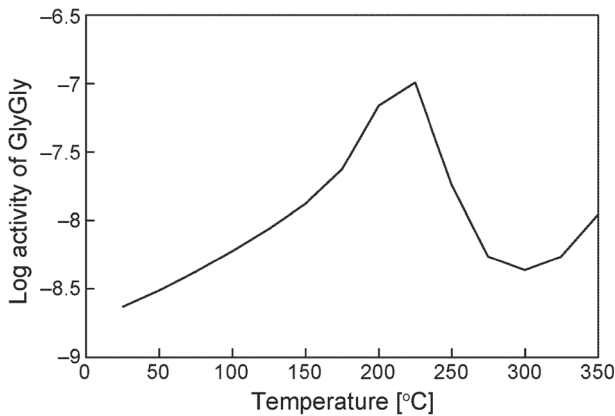


Fig. 10 Activity of GlyGly equilibrated with Gly (activity = 0.001) calculated assuming the temperature and pH conditions depicted in Fig. 6

acid polymerizations (Huber and Wachtershauser 1998; Huber et al. 2003; Milner-White and Russell 2011; Bianchi et al. 2012), provided amino acids can be sufficiently concentrated. (Fe,Ni)S compartments therefore could have supported both the generation and polymerization of amino acids. A concern of this model is whether amino acids can be accumulated sufficiently within the compartments to produce sufficient concentration of peptides to support the origin and early evolution of life. Future investigation of the (Fe,Ni)S–amino acid interaction (e.g. adsorption) is expected to be helpful not only to estimate the concentrations but also to constrain possible combinations of amino acids necessary for the complexification of organic materials for the origin of life.

Conclusion

A complete set of the standard molal thermodynamic data and the revised HKF parameters for the 20 protein amino acids are described as results of this study (Table 1). The dataset enabled prediction of the thermodynamic behaviors of the protein amino acids over broad ranges of temperature and pH. As a test to ascertain whether the alkaline hydrothermal system is favorable or not for abiotic synthesis of amino acids, the author calculated the $\Delta_r G$ necessary to synthesize the 20 protein amino acids from inorganic precursors (CO_2 , H_2 , NH_3 , and H_2S) under a simulated alkaline hydrothermal system on the Hadean Earth. Results showed that the mixing between the CO_2 -rich seawater and the H_2 -rich hydrothermal fluid can produce energetically favorable conditions for the amino acid syntheses, particularly in the lower-temperature region of such systems. The mixing was also expected to provide favorable conditions for the polymerization of amino acids, but the optimum temperature (about 225 °C) was much higher than those for the amino acid syntheses (about 50 °C). The Hadean alkaline hydrothermal setting presumably provided steep pH and temperature gradients between cool, slightly acidic CO_2 -rich Hadean Ocean and hot, alkaline hydrothermal fluids rich in H_2 , NH_3 , and H_2S at the vent–ocean interface, as simulated in the mixing calculation. That setting is an energetically excellent environment for amino acid synthesis and polymerization.

Acknowledgments This manuscript was significantly improved owing to many helpful comments and suggestions of two anonymous reviewers. This research was financially supported by the World Premier International Research Center Initiative (WPI).

Appendix A

Standard State Conventions

The standard state convention adopted for H₂O is unit activity of the pure solvent at any temperature and pressure. The convention for other aqueous species corresponds to the unit activity of the species in a hypothetical one molal solution referenced to infinite dilution at any temperature or pressure. The conventional standard molal thermodynamic properties of a charged aqueous species are given as the following.

$$\Xi = \Xi^{abs} - Z\Xi_{H^+}^{abs} \quad (A1)$$

Therein, Ξ and Ξ^{abs} respectively stand for any conventional and absolute standard molal properties of the aqueous species of interest. $\Xi_{H^+}^{abs}$ signifies the corresponding absolute standard molal property of the hydrogen ion. In addition, Z represents the charge of the aqueous species of interest.

The standard molal Gibbs energies (ΔG^o) and enthalpies (ΔH^o) of aqueous species are expressed as apparent standard molal Gibbs energies and enthalpies of formation, which are defined as

$$\Delta H^o \equiv \Delta_f H^o + \left(H_{P,T}^o - H_{P_r,T_r}^o \right) \quad (A2)$$

and

$$\Delta G^o \equiv \Delta_f G^o + \left(G_{P,T}^o - G_{P_r,T_r}^o \right) \quad (A3)$$

where $\Delta_f G^o$ and $\Delta_f H^o$ represent the standard molal Gibbs energy and enthalpy of formation of the species from the elements at the reference temperature ($T_r=298.15$ K) and pressure ($P_r=1$ bar), and where $G_{P,T}^o - G_{P_r,T_r}^o$ and $H_{P,T}^o - H_{P_r,T_r}^o$ respectively denote the differences between the standard molal Gibbs energy and enthalpy at the temperature (T) and pressure (P) of interest, and those at T_r and P_r .

The values of $\Delta_f G^o$ and $\Delta_f H^o$ and the standard molal entropy at 25 °C and 1 bar (S_{P_r,T_r}^o) are related to the following.

$$\Delta G_f^o = \Delta H_f^o - T_r \left(S_{P_r,T_r}^o - S_{P_r,T_r,elements}^o \right) \quad (A4)$$

In that equation, $S_{P_r,T_r,elements}^o$ represents the total standard molal entropy at 25 °C and 1 bar of the elements making up the species of interest. The values of S_{P_r,T_r}^o of the elements used for this study were referred from a report by Cox et al. (1989).

Summary of the Revised HKF Equation of State

The revised HKF equations of state are consistent with the separation of variables shown below.

$$\Xi = \Delta\Xi_n + \Delta\Xi_s \quad (A5)$$

Therein, Ξ stands for any standard molal property of an aqueous species. In addition, $\Delta\Xi_n$ and $\Delta\Xi_s$ respectively refer to the nonsolvation and solvation contributions to Ξ .

The nonsolvation contributions to the standard molal isobaric heat capacity (C_P°), volume (V°) and isothermal compressibility (κ_T°) of an aqueous species ($\Delta C_{P,n}^\circ$, ΔV_n° , and $\Delta \kappa_{T,n}^\circ$, respectively) are given in the literature (Tanger and Helgeson 1988) as

$$\Delta C_{P,n}^\circ = c_1 + \frac{c_2}{(T-\Theta)^2} \left(\frac{2T}{(T-\Theta)^3} \right) \left(a_3(P-P_r) + a_4 \ln \left(\frac{\Psi + P}{\Psi + P_r} \right) \right) \tag{A6}$$

$$\Delta V_n^\circ = a_1 + \frac{a_2}{\Psi + P} \left(a_3 + \frac{a_4}{\Psi + P} \right) \left(\frac{1}{T-\Theta} \right) \tag{A7}$$

and

$$\Delta \kappa_{T,n}^\circ = \left(a_2 + \frac{a_4}{T-\Theta} \right) \left(\frac{1}{\Psi + P} \right)^2 \tag{A8}$$

where a_1 , a_2 , a_3 , a_4 , c_1 , and c_2 represent temperature-independent and pressure-independent parameters of the species of interest, and where Θ and Ψ respectively represent solvent parameters equal to 228 K and 2600 bar.

The solvation contributions to C_P° , V° , and κ_T° are expressed as

$$\Delta C_{P,s}^\circ = \omega TX + 2TY \left(\frac{\partial \omega}{\partial T} \right)_P - T \left(\frac{1}{\epsilon} - 1 \right) \left(\frac{\partial^2 \omega}{\partial T^2} \right)_P \tag{A9}$$

$$\Delta V_s^\circ = \omega Q + \left(\frac{1}{\epsilon} - 1 \right) \left(\frac{\partial \omega}{\partial P} \right)_T \tag{A10}$$

and

$$\Delta \kappa_{T,s}^\circ = \omega N + 2Q \left(\frac{\partial \omega}{\partial P} \right)_T - \left(\frac{1}{\epsilon} - 1 \right) \left(\frac{\partial^2 \omega}{\partial P^2} \right)_T \tag{A11}$$

where ω denotes the solvation parameter of the species of interest, ϵ stands for the dielectric constant of H₂O, and Q , N , Y , and X represent the Born functions defined respectively as $-\left(\frac{\partial(1/\epsilon)}{\partial P} \right)_T$, $\left(\frac{\partial Q}{\partial P} \right)_T$, $-\left(\frac{\partial(1/\epsilon)}{\partial T} \right)_P$, and $\left(\frac{\partial Y}{\partial T} \right)_P$. The values of Q , N , and Y used for this study were taken from Shock et al. (1992), but those of N correspond to the values reported by Tanger and Helgeson (1988). The partial derivatives of ω with respect to temperature and pressure are taken as

$$\left(\frac{\partial \omega}{\partial T} \right)_P = \left(\frac{\partial \omega}{\partial P} \right)_T = \left(\frac{\partial^2 \omega}{\partial T^2} \right)_P = \left(\frac{\partial^2 \omega}{\partial P^2} \right)_T = 0 \tag{A12}$$

for all the neutral and charged groups and species considered below (Amend and Helgeson 1997, 2000; Dick et al. 2006).

At $P \approx P_r$, Eq. (A6) reduces to the equation presented below.

$$\Delta C_{P,n}^\circ = c_1 + \frac{c_2}{(T-\Theta)^2} \tag{A13}$$

Contributions by the pressure-dependent terms are negligible for pressures of less than a few hundred bar (Dick et al. 2006). Eq. (A7) can be written as

$$\Delta V_n^o = \sigma + \frac{\xi}{T-\Theta} \quad (\text{A14})$$

by defining the parameters σ and ξ as

$$\sigma \equiv a_1 + \frac{a_2}{\Psi + P} \quad (\text{A15})$$

and the following expression.

$$\xi \equiv a_3 + \frac{a_4}{\Psi + P} \quad (\text{A16})$$

By taking account of Eqs. (A5) and (A12) together with Eqs. (A9) and (A13) for C_P^o or Eqs. (A10) and (A14) for V^o , it is possible to write

$$C_P^o = c_1 + \frac{c_2}{(T-\Theta)^2} + \omega TX \quad (\text{A17})$$

and the following.

$$V^o = \sigma + \frac{\xi}{T-\Theta} - \omega Q \quad (\text{A18})$$

The revised HKF equations of state for ΔG^o , ΔH^o , and S^o can be written as (Tanger and Helgeson 1988)

$$\begin{aligned} \Delta G^o = & \Delta G_f^o - S_{P_r, T_r}^o (T - T_r) - c_1 \left[T \ln \left(\frac{T}{T_r} \right) - T + T_r \right] - c_2 \left\{ \left[\left(\frac{1}{T-\Theta} \right) - \left(\frac{1}{T_r-\Theta} \right) \right] \left(\frac{\Theta-T}{\Theta} \right) \right\} \\ & + c_2 \left\{ \frac{T}{\Theta^2} \ln \left[\frac{T_r(T-\Theta)}{T(T_r-\Theta)} \right] \right\} + a_1(P-P_r) + a_2 \ln \left(\frac{\Psi+P}{\Psi+P_r} \right) \\ & + \left(\frac{1}{T+\Theta} \right) \left[a_3(P-P_r) + a_4 \ln \left(\frac{\Psi+P}{\Psi+P_r} \right) \right] \\ & + \omega \left(\frac{1}{\epsilon} - 1 \right) - \omega_{P_r, T_r} \left[Y_{P_r, T_r}(T_r - T) + \frac{1}{\epsilon_{P_r, T_r}} - 1 \right] \end{aligned} \quad (\text{A19})$$

$$\begin{aligned} \Delta H^o = & \Delta H_f^o + c_1(T - T_r) - c_2 \left[\left(\frac{1}{T-\Theta} \right) - \left(\frac{1}{T_r-\Theta} \right) \right] + a_1(P - P_r) + a_2 \ln \left(\frac{\Psi+P}{\Psi+P_r} \right) \\ & + \left[\frac{2T-\Theta}{(T-\Theta)^2} \right] \left[a_3(P - P_r) + a_4 \ln \left(\frac{\Psi+P}{\Psi+P_r} \right) \right] \\ & + \omega \left(TY + \frac{1}{\epsilon} - 1 \right) - T \left(\frac{1}{\epsilon} - 1 \right) \left(\frac{\partial \omega}{\partial T} \right)_P - \omega_{P_r, T_r} \left(T_r Y_{P_r, T_r} + \frac{1}{\epsilon_{P_r, T_r}} - 1 \right) \end{aligned} \quad (\text{A20})$$

and

$$\begin{aligned}
S^o = & S_{P_r, T_r}^o + c_1 \ln \left(\frac{T}{T_r} \right) - \frac{c_2}{\Theta} \left\{ \left(\frac{1}{T-\Theta} \right) - \left(\frac{1}{T_r-\Theta} \right) + \frac{1}{\Theta} \ln \left[\frac{T_r(T-\Theta)}{T(T_r-\Theta)} \right] \right\} \\
& + \left(\frac{1}{T-\Theta} \right)^2 \left[a_3(P-P_r) + a_4 \ln \left(\frac{\Psi+P}{\Psi+P_r} \right) \right] \\
& + \omega Y - \left(\frac{1}{\epsilon} - 1 \right) \left(\frac{\partial \omega}{\partial T} \right)_P^{-\omega_{P_r, T_r} Y_{P_r, T_r}} \quad (A21)
\end{aligned}$$

respectively.

Appendix B

Based on group additivity algorithms developed by Amend and Helgeson (1997, 2000) and Dick et al. (2006), thermodynamic properties of an amino acid are separable into two contributions as shown below.

$$\bar{\Xi}_{AA} = \bar{\Xi}_{[AABB]} + \bar{\Xi}_{[SC]} \quad (B1)$$

Therein, $\bar{\Xi}_{AA}$, $\bar{\Xi}_{[AABB]}$, and $\bar{\Xi}_{[SC]}$ respectively stand for any thermodynamic data or revised HKF parameters for the amino acid, amino acid backbone, and side-chain group. Depending on the protonation state of functional groups in the amino acid structure, the amino acid backbone and the side-chain group have positive, neutral, or negative charge (e.g., $[AABB^-] + 2H^+ \leftrightarrow [AABB] + H^+ \leftrightarrow [AABB^+]$). The data and parameters for $[AABB]$, $[AABB^-]$, $[AABB^+]$, and all side-chain groups of the 20 protein amino acids have been reported by Dick et al. (2006). However, the parameters for $[AABB^+]$ and $[AABB^-]$ were calculated using the corresponding values for single amino acid by combination with those for $[AABB]$ (e.g., a_1 , a_2 , a_3 , a_4 , c_1 , c_2 , and ω for $[AABB^-]$ were calculated from $\bar{\Xi}_{[AABB^-]} = \bar{\Xi}_{[AABB]} + \bar{\Xi}_{Lys^-} - \bar{\Xi}_{Lys}$) because of the paucity of available thermodynamic properties of charged amino acids at the time. The data and parameters for $[Lys]$ and $[Arg]$ were then retrieved from corresponding values of Lys^- and Arg^- by subtracting the contribution of $[AABB^-]$ (e.g., $\bar{\Xi}_{[Lys]} = \bar{\Xi}_{Lys^-} - \bar{\Xi}_{[AABB^-]}$). Similarly, the data and parameters for $[Arg^+]$, $[Asp^-]$, $[Cys^-]$, $[Glu^-]$, $[His^+]$, $[Lys^+]$, $[Tyr^-]$ were calculated using the values of corresponding amino acids together with those of $[AABB]$ (e.g., $\bar{\Xi}_{[Arg^+]} = \bar{\Xi}_{Arg^+} - \bar{\Xi}_{[AABB]}$). Because many thermodynamic properties of charged amino acids were updated in this study, the values for the compounds described above were recalculated in the manner described below.

First, the data and parameters for $[Arg^+]$, $[Asp^-]$, $[Cys^-]$, $[Glu^-]$, $[His^+]$, $[Lys^+]$ were calculated using the corresponding values for $[AABB]$ given by Dick et al. (2006) together with those for the amino acids presented in Table 1 from the following, as

$$\bar{\Xi}_{[SC^+]} = \bar{\Xi}_{AA^+} - \bar{\Xi}_{[AABB]} \quad (B2)$$

for $[Arg^+]$, $[His^+]$, $[Lys^+]$, and

$$\bar{\Xi}_{[SC^-]} = \bar{\Xi}_{AA^-} - \bar{\Xi}_{[AABB]} \quad (B3)$$

for $[Asp^-]$, $[Cys^-]$, $[Glu^-]$.

Second, the data and parameters for Ala^+ , Arg^{2+} , Asn^+ , Asp^+ , Cys^+ , Gln^+ , Glu^+ , Gly^+ , His^{2+} , Ile^+ , Leu^+ , Lys^{2+} , Met^+ , Phe^+ , Ser^+ , Thr^+ , Trp^+ , Tyr^+ , and Val^+ presented in Table 1 were correlated with the corresponding values for $[Ala]$, $[Arg^+]$, $[Asn]$, $[Asp]$, $[Cys]$, $[Gln]$, $[Glu]$,

[Gly], [His⁺], [Ile], [Leu], [Lys⁺], [Met], [Phe], [Ser], [Thr], [Trp], [Tyr], and [Val] reported by Dick et al. (2006), except for [Met], [Arg⁺], [His⁺], and [Lys⁺], which were taken from LaRowe and Dick (2012) for [Met], and which were calculated from Eq. (B2) for [Arg⁺], [His⁺], and [Lys⁺] (Fig. 11a–l). The values for Pro were not included in this figure because Pro has the imino group instead of the amino group. It follows from Eq. (B1) that the intercepts of the regression lines (slopes = 1) shown in Fig. 11a–l correspond to the data and parameters for [AABB⁺]. Because no linear relation was observed for a_3 and ω (Fig. 11h and l), these were calculated from Eq. (A17) and (A18) using the values retrieved from the correlation depicted in Fig. 11. The value of S° at 25 °C and 1 bar for [AABB⁺] was calculated from Eq. (A4) using the values of $\Delta_r G^\circ$ and $\Delta_r H^\circ$ obtained using the procedure described above together with values of S° for elements taken from Cox et al. (1989). Similarly, the data and parameters for Ala⁻, Asn⁻, Asp²⁻, Cys²⁻, Gln⁻, Glu²⁻, Gly⁻, His⁻, Ile⁻, Leu⁻, Met⁻, Phe⁻, Ser⁻, Thr⁻, Trp⁻, Tyr⁻, and Val⁻ presented in Table 1 were correlated with the corresponding values for [Ala], [Asn], [Asp⁻], [Cys⁻], [Gln], [Glu⁻], [Gly], [His], [Ile], [Leu], [Met], [Phe], [Ser], [Thr], [Trp], [Tyr], and [Val] reported by Dick et al. (2006), except for [Asp⁻], [Cys⁻], and [Glu⁻], which was calculated from Eq. (B3) (Fig. 11m–x). All values except for S° at 25 °C and 1 bar, a_3 , and ω were retrieved from the intercepts of the regression lines depicted in Fig. 11m–x, whereas the three properties were calculated from Eqs. (A17), (A18), and (A4) using the retrieved values.

The data and parameters for [AABB⁻] were then used to calculate those of [Lys], [Arg], and [Tyr⁻] as the following.

$$\Xi_{[Lys]} = \Xi_{Lys^-} - \Xi_{[AABB^-]} \quad (B4)$$

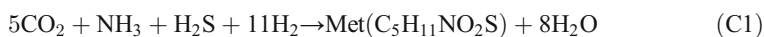
$$\Xi_{[Arg]} = \Xi_{Arg^-} - \Xi_{[AABB^-]} \quad (B5)$$

$$\Xi_{[Tyr^-]} = \Xi_{Tyr^{2-}} - \Xi_{[AABB^-]} \quad (B6)$$

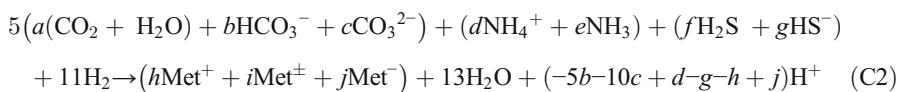
The data and parameters obtained through the procedure described above are presented in Table 3.

Appendix C

In this appendix, the calculation procedure of $\Delta_r G_{pH}^\circ$ is described using the synthesis reaction of Met from CO₂ (H₂CO₃ is the actual dissolved structure of CO₂ in aqueous solution), NH₃, H₂S, and H₂ as a model. The reaction is written as



Among the components in this equation, H₂CO₃, NH₃, H₂S, and Met change its speciation depending on the temperature and pH. The speciation changes can be incorporated by rewriting the equation as presented below.



Therein, the italic characters denote the mole fractions of respective species ($a+b+c=d+e=h+i+j=1$). H⁺ was added at the right side of the equation to maintain the charge balance. By combining the equation with Eq. (10), (11), and (12), the Gibbs

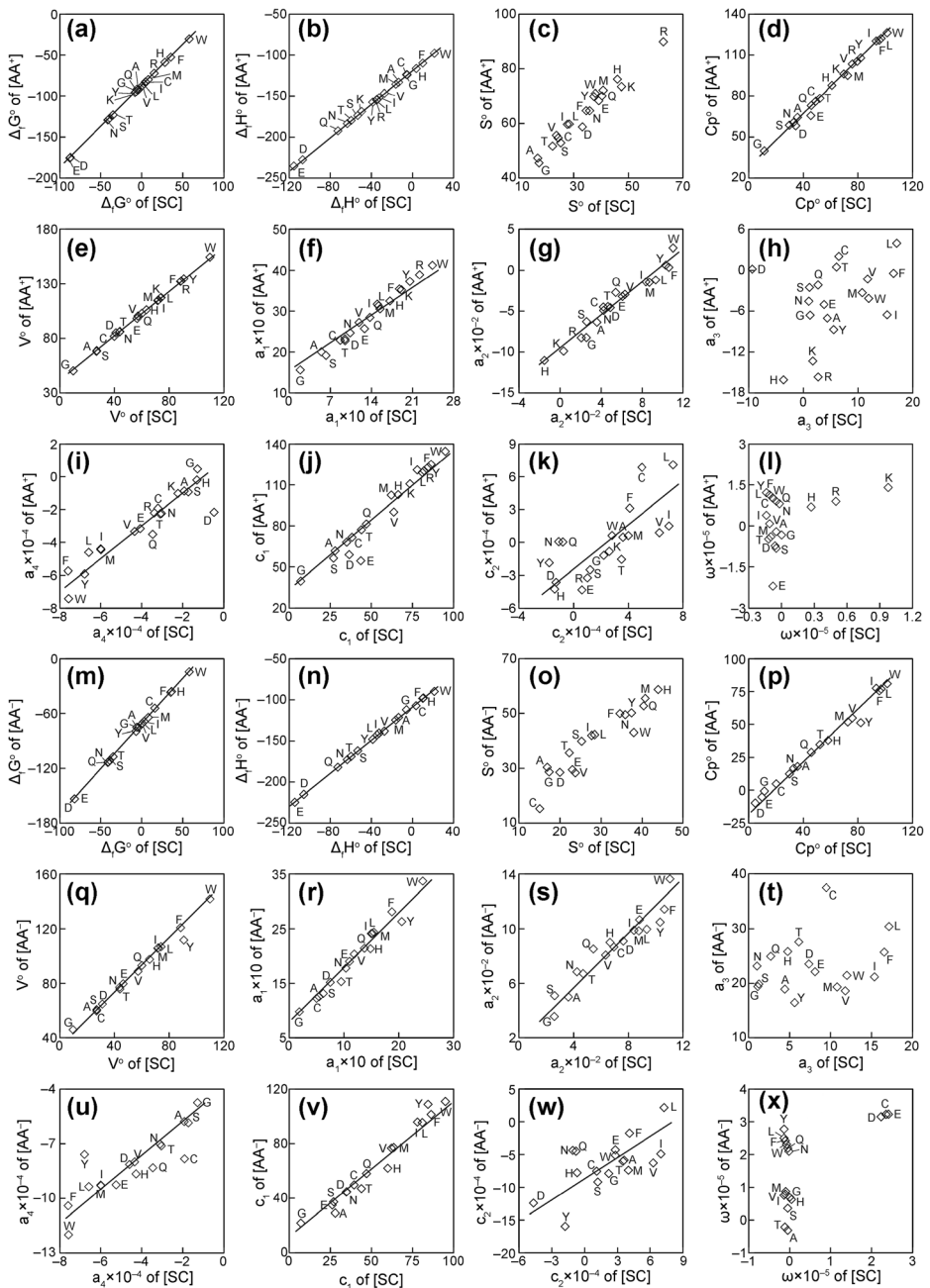


Fig. 11 Correlations of the thermodynamic data and the revised HKF parameters between amino acids and corresponding side-chain groups. Regression lines have slopes of unity and intercepts that correspond to the data and parameters for [AABB⁻] and [AABB]

energy necessary to synthesize Met from the inorganic precursors at a given pH, $\Delta_r G_{pH}^\circ$, is represented by the following equation.

Table 3 Standard molal thermodynamic data at 25 °C and 1 bar and revised HKF equation of state parameters for several side-chain groups and amino acid backbone updated in this study

Species	$\Delta_f G^{oa}$	$\Delta_f H^{oa}$	$S^o_{Pr}; T^b$	C_p^{ob}	V^{oc}	$a_1^d \times 10$	$a_2^e \times 10^{-2}$	a_3^f	$a_4^g \times 10^{-4}$	c_l^b	$c_2^g \times 10^{-4}$	$\omega^s \times 10^{-5}$
[Arg ⁺]	30.65	-33.39	15.68	99.6	110.6	23.38	12.17	17.01	-6.27	130.4	-11.02	0.93
[Arg ⁰]	15.24	-34.65	63.00	79.6	88.9	22.25	2.08	2.69	-3.38	82.2	1.00	0.50
[Asp ⁻]	-82.51	-105.97	19.92	4.7	31.2	7.49	7.63	7.34	-4.60	34.7	-4.70	2.24
[Cys ⁻]	15.95	3.77	15.03	20.1	27.0	4.97	6.94	9.47	-1.91	39.4	1.10	2.36
[Glu ⁻]	-82.38	-114.65	22.99	9.6	46.4	11.02	8.82	8.09	-5.25	26.0	2.80	2.42
[His ⁺]	28.31	3.91	47.52	61.1	63.4	17.17	-1.54	-3.65	-1.30	66.4	-1.40	0.27
[Lys ⁺]	5.91	-39.69	31.72	91.3	79.79	20.39	8.94	-12.14	-3.94	122.2	-9.42	1.30
[Lys ⁰]	-8.21	-49.51	46.02	69.9	73.9	19.15	0.35	1.70	-2.22	73.6	2.60	0.98
[Tyr ⁻]	6.91	-27.48	28.21	33.8	69.2	16.73	11.38	5.72	-7.26	79.9	-13.15	2.11
[AABB ⁺]	-87.65	-11.97	29.56	26.1	42.6	15.02	-9.58	-10.41	0.95	33.6	-2.48	0.27
[AABB ⁻]	-71.72	-109.26	11.14	-18.5	32.4	7.82	1.64	15.67	-3.71	11.5	-8.58	1.37

^a kcal mol⁻¹, ^b cal mol⁻¹ K⁻¹, ^c cm³ mol⁻¹, ^d cal mol⁻¹ bar⁻¹, ^e cal mol⁻¹, ^f cal K mol⁻¹, ^g cal K mol⁻¹

$$\Delta_r G_{pH}^o = \Delta_r G^o + (-5b-10c+d-g-h+j)RT \ln 10^{-pH} \quad (C3)$$

The mole fractions at any temperature and pH are calculable using the protonation constant of respective species as the following.

$$a = \frac{\frac{K_{HCO_3} a_{H^+}}{\gamma_{CO_2}}}{\frac{1}{\gamma_{CO_3^-} K_{CO_3} a_{H^+}} + \frac{1}{\gamma_{HCO_3^-}} + \frac{K_{HCO_3} a_{H^+}}{\gamma_{CO_2}}} \quad (C4)$$

$$b = \frac{\frac{1}{\gamma_{HCO_3^-}}}{\frac{1}{\gamma_{CO_3^-} K_{CO_3} a_{H^+}} + \frac{1}{\gamma_{HCO_3^-}} + \frac{K_{HCO_3} a_{H^+}}{\gamma_{CO_2}}} \quad (C5)$$

$$c = 1-a-b \quad (C6)$$

$$d = \frac{\frac{K_{NH_3} a_{H^+}}{\gamma_{NH_4^+}}}{\frac{1}{\gamma_{NH_3}} + \frac{K_{NH_3} a_{H^+}}{\gamma_{NH_4^+}}} \quad (C7)$$

$$e = 1-d \quad (C8)$$

$$f = \frac{\frac{K_{HS^-} a_{H^+}}{\gamma_{H_2S}}}{\frac{1}{\gamma_{HS^-}} + \frac{K_{HS^-} a_{H^+}}{\gamma_{H_2S}}} \quad (C9)$$

$$g = 1-f \quad (C10)$$

$$h = \frac{\frac{K_{Mer^{\pm}} a_{H^+}}{\gamma_{Mer^+}}}{\frac{1}{\gamma_{Mer^-} K_{Mer} a_{H^+}} + \frac{1}{\gamma_{Mer^{\pm}}} + \frac{K_{Mer^{\pm}} a_{H^+}}{\gamma_{Mer^+}}} \quad (C11)$$

$$i = \frac{\frac{1}{\gamma_{Mer^{\pm}}}}{\frac{1}{\gamma_{Mer^-} K_{Mer} a_{H^+}} + \frac{1}{\gamma_{Mer^{\pm}}} + \frac{K_{Mer^{\pm}} a_{H^+}}{\gamma_{Mer^+}}} \quad (C12)$$

$$j = 1-h-i \quad (C13)$$

Therein, K_i represents protonation constants of the species i at any temperature and pressure calculated from Eq. (9) using thermodynamic data and the revised HKF

parameters presented by Shock et al. (1989, 1997) for HCO_3^- , CO_3^{2-} , NH_3 , HS^- , and those presented in Table 1 for Met^+ and Met^- . In addition, γ_i stand for the activity coefficient of the species i calculated using the extended Debye–Huckel equation (Helgeson et al. 1981). The values of $\Delta_r G_{pH}^o$ for the other amino acids were calculated in the same manner as those described above.

References

- Amend JP, Helgeson HC (1997) Calculation of the standard molal thermodynamic properties of aqueous biomolecules at elevated temperatures and pressures. Part 1. L- α -amino acids. *J Chem Soc Faraday Trans* 93:1927–1941
- Amend JP, Helgeson HC (2000) Calculation of the standard molal thermodynamic properties of aqueous biomolecules at elevated temperatures and pressures. II. Unfolded proteins. *Biophys Chem* 84:105–136
- Amend JP, McCollom TM (2009) Energetics of biomolecule synthesis on early earth. In: Zaikowski L, Friedrich JM, Seidel SR (eds) *Chemical evolution II: from the origins of life to modern society*, American chemical society symposium series. Oxford University Press, New York, pp 63–94
- Amend JP, Shock EL (1998) Energetics of amino acid synthesis in hydrothermal ecosystems. *Science* 281:1659–1662
- Anderson KP, Greenhalgh WO, Izatt RM (1966) Formation constants and enthalpy and entropy values for the association of H^+ and Cu^{2+} with glycinate and phenylalanate ions in aqueous solution at 10, 25, and 40°. *Inorg Chem* 5:2106–2109
- Anderson KP, Greenhalgh WO, Butler EA (1967) Formation constant, enthalpy, and entropy values for the association of nickel(II) ion with glycinate, alanate, and phenylalanate ions at 10, 25, and 40°. *Inorg Chem* 6: 1056–1058
- Bada JL (2004) How life began on Earth: a status report. *Earth Planet Sci Lett* 226:1–15
- Bada JL, Bigham C, Miller SL (1994) Impact melting of frozen oceans on the early Earth: implications for the origin of life. *Proc Natl Acad Sci U S A* 91:1248–1250
- Barge LM, Kee TP, Doloboff IJ, Hampton JMP, Ismail M, Pourkashanian M, Zeytounian J, Baum MM, Moss JA, Lin CK, Kidd RD, Kanik I (2014) The fuel cell model of abiogenesis: a new approach to origin-of-life simulations. *Astrobiology* 14:254–270
- Baross JA, Hoffman SE (1985) Submarine hydrothermal vents and associated gradient environments as sites for the origin and evolution of life. *Orig Life* 15:327–345
- Bernhardt HS, Tate WP (2012) Primordial soup or vinaigrette: did the RNA world evolve at acidic pH? *Biol Direct* 7:4
- Bianchi A, Giorgi C, Ruzza P, Toniolo C, Milner-White EJ (2012) A synthetic hexapeptide designed to resemble a proteinaceous p-loop nest is shown to bind inorganic phosphate. *Proteins Struct Funct Bioinforma* 80: 1418–1424
- Clarke RGF, Collins CM, Roberts JC, Trevani LN, Bartholomew RJ, Tremaine PR (2005) Ionization constants of aqueous amino acids at temperatures up to 250°C using hydrothermal pH indicators and UV–visible spectroscopy: glycine, α -alanine, and proline. *Geochim Cosmochim Acta* 69:3029–3043
- Coates E, Marsden CG, Rigg B (1969) Ionization of cysteine in aqueous solutions part 2.—specific-ionization constants. *Trans Faraday Soc* 65:3032–3036
- Corliss JB, Baross JA, Hoffman SE (1981) An hypothesis concerning the relationship between submarine hot springs and the origin of life on Earth. *Oceanol Acta SP*, 59–69
- Cox JD, Wagman DD, Medvedev VA (1989) COVATA key values for thermodynamics. Hemisphere Publishing Corporation, New York
- Dick JM, LaRowe DE, Helgeson HC (2006) Temperature, pressure, and electrochemical constraints on protein speciation: group additivity calculation of the standard molal thermodynamic properties of ionized unfolded proteins. *Biogeosciences* 3:311–336
- Doring A, Schulzke C (2010) Tungsten’s redox potential is more temperature sensitive than that of molybdenum. *Dalton Trans* 39:5623–5629
- Emmanuel S, Berkowitz B (2006) Suppression and stimulation of seafloor hydrothermal convection by exothermic mineral hydration. *Earth Planet Sci Lett* 243:657–668
- Gergely A, Mojzes J, Kassai-Bazsa ZS (1972) Equilibrium relations of alpha-amino acid complexes of transition metal ions—V Stability constants and formation enthalpy and entropy changes of complexes of serine, threonine and alpha-aminobutyric acid. *J Inorg Nucl Chem* 34:1277–1290

- Gilbert W (1986) The RNA world. *Nature* 319:618
- Gillespie SE, Oscarson JL, Izatt RM, Wang P, Renuncio JAR, Pando C (1995) Thermodynamic quantities for the protonation of amino acid amino groups from 323.15 to 398.15 K. *J Sol Chem* 24:1219–1247
- Goldberg RN, Kishore N, Lennen RM (2002) Thermodynamic quantities for the ionization reactions of buffers. *J Phys Chem Ref Data* 31:231–370
- Hamborg ES, Niederer PM, Versteeg GF (2007) Dissociation constants and thermodynamic properties of amino acids used in CO₂ absorption from (293 to 353) K. *J Chem Eng Data* 52:2491–2502
- Helgeson HC, Kirkham DH (1974) Theoretical prediction of the thermodynamic behavior of aqueous electrolytes at high pressures and temperatures: I. summary of the thermodynamic/electrostatic properties of the solvent. *Am J Sci* 274:1089–1198
- Helgeson HC, Delany JM, Nesbitt HW, Bird DK (1978) Summary and critique of the thermodynamic properties of rock-forming minerals. *Am J Sci* 278A:1–229
- Helgeson HC, Kirkham DH, Flowers GC (1981) Theoretical prediction of the thermodynamic behavior of aqueous electrolytes at high pressures and temperatures: IV. Calculation of activity coefficients, osmotic coefficients, and apparent molal and standard and relative partial molal properties to 600 °C and 5 kb. *Am J Sci* 281:1249–1516
- Helz GR, Erickson BE, Vorlicek TP (2014) Stabilities of thiomolybdate complexes of iron; implications for retention of essential trace elements (Fe, Cu, Mo) in sulfide waters. *Metallomics* 6:1131–1140
- Huber C, Wächtershäuser G (1998) Peptides by activation of amino acids with CO on (Ni, Fe)S surfaces: Implications for the origin of life. *Science* 281:670–672
- Huber C, Wächtershäuser G (2006) α -hydroxy and α -amino acids under possible hadean, volcanic origin-of-life conditions. *Science* 314:630–632
- Huber C, Eisenreich W, Hecht S, Wächtershäuser G (2003) A possible primordial peptide cycle. *Science* 301: 938–940
- Humbolt V, Methivier C, Pradier CM (2006) Adsorption of L-lysine on Cu(110): A RAIRS study from UHV to liquid phase. *Langmuir* 22:3089–3096
- Izatt RM, Wrathall JW, Anderson KP (1961) Studies of the copper(II)–alanine and phenylalanine systems in aqueous solution. Dissociation and formation constants as a function of temperature. *J Phys Chem* 65:1914–1915
- Izatt RM, Christensen JJ, Kothari V (1964) Acid dissociation constant, formation constant, enthalpy, and entropy values for some copper(II)– α -amino acid systems in aqueous solution. *Inorg Chem* 3:1565–1567
- Jardine JJ, Call TG, Patterson BA, Origlia-Luster ML, Woolley EM (2001) Thermodynamics for proton dissociations from aqueous L-histidine at temperatures from 278.15 K to 393.15 K and at the pressure 0.35 MPa: apparent molar volumes and apparent molar heat capacities of the protonated cationic, neutral zwitterionic, and deprotonated anionic forms. *J Chem Thermodyn* 33:1419–1440
- Joyce GF (2002) The antiquity of RNA-based evolution. *Nature* 418:214–221
- Kelley DS, Karson JA, Blackman DK, Fruh-Green GL, Butterfield DA, Lilley MD, Olson EJ, Schrenk MO, Roe KK, Lebon GT, Rivizzigno P, the AT3–60 Shipboard Party (2001) An off-axis hydrothermal vent field near the Mid-Atlantic Ridge at 30°N. *Nature* 412:145–149
- Kelley DS, Karson JA, Fruh-Green GL, Yoerger DR, Shank TM, Butterfield DA, Hayes JM, Schrenk MO, Olson EJ, Proskurowski G, Jakuba M, Bradley A, Larson B, Ludwig K, Glickson D, Buckman K, Bradley AS, Brazelton WJ, Roe K, Elend MJ, Delacour A, Bernasconi SM, Lilley MD, Baross JA, Summons RE, Sylva SP (2005) A serpentine-hosted ecosystem: the lost city hydrothermal field. *Science* 307:1428–1434
- Kitadai N (2014) Thermodynamic prediction of glycine polymerization as a function of temperature and pH consistent with experimentally obtained results. *J Mol Evol* 78:171–187
- Kochergina LA, Grosheva SG, Krutova ON (2011) Thermochemical study of acid–base interactions in L-asparagine aqueous solutions. *Russ J Inorg Chem* 56:1481–1486
- Kochergina LA, Lytkin AI, Krutova ON (2013) Influence of temperature on the heats of acid–base reactions in L-glutamine aqueous solution. *Russ J Inorg Chem* 58:744–748
- Konn C, Charlou JL, Donval JP, Holm NG, Dehairs F, Bouillon S (2009) Hydrocarbons and oxidized organic compounds in hydrothermal fluids from Rainbow and Lost City ultramafic-hosted vents. *Chem Geol* 258: 299–314
- LaRowe DE, Dick JM (2012) Calculation of the standard molal thermodynamic properties of crystalline peptides. *Geochim Cosmochim Acta* 80:70–91
- LaRowe DE, Van Cappellen P (2011) Degradation of natural organic matter: a thermodynamic analysis. *Geochim Cosmochim Acta* 75:2030–2042
- Li Y, Breaker RR (1999) Kinetics of RNA degradation by specific base catalysis of transesterification involving the 2'-hydroxyl group. *J Am Chem Soc* 121:5364–5372
- Lowell RP, Rona PA (2002) Seafloor hydrothermal systems driven by the serpentinization of peridotite. *Geophys Res Lett* 29:1531

- Macleod G, McKeown C, Hall AJ, Russell MJ (1994) Hydrothermal and oceanic pH conditions of possible relevance to the origin of life. *Orig Life Evol Biosph* 24:19–41
- Marcus Y (1994) A simple empirical model describing the thermodynamics of hydration of ions of widely varying charges, sizes, and shapes. *Biophys Chem* 51:111–127
- Martell AE, Smith RM (1982) Critical stability constants, vol 5. Plenum Press, New York, p 604
- Martin B, Fyfe WS (1970) Some experimental and theoretical observations on kinetics of hydration reactions with particular reference to serpentinization. *Chem Geol* 6:185–202
- Martin W, Russell MJ (2007) On the origin of biochemistry at an alkaline hydrothermal vent. *Phil Trans R Soc B* 362:1887–1925
- Martin W, Baross J, Kelley D, Russell MJ (2008) Hydrothermal vents and the origin of life. *Microbiology* 6:805–814
- McCullom TM, Amend JP (2005) A thermodynamic assessment of energy requirements for biomass synthesis by chemolithoautotrophic micro-organisms in oxic and anoxic environments. *Geobiology* 3:135–144
- McCullom TM, Seewald JS (2003) Experimental constraints on the hydrothermal reactivity of organic acids and acid anions: I. Formic acid and formate. *Geochim Cosmochim Acta* 67:3625–3644
- McCullom TM, Seewald JS (2007) Abiotic synthesis of organic compounds in deep-sea hydrothermal environments. *Chem Rev* 107:382–401
- McCullom TM, Seewald JS (2013) Serpentinites, hydrogen, and life. *Elements* 9:129–134
- McCullom TM, Shock EL (1997) Geochemical constraints on chemolithoautotrophic metabolism by microorganisms in seafloor hydrothermal systems. *Geochim Cosmochim Acta* 61:4375–4391
- Milner-White EJ, Russell MJ (2011) Functional capabilities of the earliest peptides and the emergence of life. *Genes* 2:671–688
- Morse JW, Mackenzie FT (1998) Hadean Ocean carbonate geochemistry. *Aquat Geochem* 4:301–319
- Nagai H, Kuwabara K, Carta G (2008) Temperature dependence of the dissociation constants of several amino acids. *J Chem Eng Data* 53:619–627
- Nakamura R, Takashima T, Kato S, Takai K, Yamamoto M, Hashimoto K (2010) Electrical current generation across a black smoker chimney. *Angew Chem Int Ed* 49:7692–7694
- Price JL, Jardine JJ, Call TG, Patterson BA, Origlia-Luster ML, Woolley EM (2003a) Thermodynamics for proton dissociations from aqueous L-histidine at temperatures from 278.15 to 393.15 K and at the pressure 0.35 MPa: apparent molar volumes and apparent molar heat capacities of the protonated cationic, neutral zwitterionic, and deprotonated anionic forms. *J Chem Thermodyn* 35:195–198
- Price JL, Sorenson EC, Merkley ED, McRae BR, Woolley EM (2003b) Thermodynamics for proton dissociations from aqueous L-valine and L-2-amino-n-butanoic acid: apparent molar volumes and apparent molar heat capacities of the protonated cationic, neutral zwitterionic, and deprotonated anionic species at temperatures from 278.15 ≤ T/K ≤ 393.15, at molalities 0.015 ≤ m/mol·kg⁻¹ ≤ 0.67, and pressure p = 0.35 MPa. *J Chem Thermodyn* 35:1425–1467
- Proskurowski G, Lille MD, Seewald JS, Fruh-Green GL, Olson EJ, Lupton JE, Sylva SP, Kelley DS (2008) Abiogenic hydrocarbon production at Lost City hydrothermal field. *Science* 319:604–607
- Rodante F (1989) Thermodynamics of the “standard” α-amino acids in water at 25 °C. *Thermochim Acta* 149:157–171
- Rode BM (1999) Peptides and the origin of life. *Peptides* 20:773–786
- Russell MJ (2003) The importance of being alkaline. *Science* 302:580–581
- Russell MJ (2007) The alkaline solution to the emergence of life: energy, entropy and early evolution. *Acta Biotheor* 55:133–179
- Russell MJ, Hall AJ (1997) The emergence of life from iron monosulphide bubbles at a submarine hydrothermal redox and pH front. *J Geol Soc Lond* 154:377–402
- Russell MJ, Martin W (2004) The rocky roots of the acetyl-CoA pathway. *Trends Biochem Sci* 29:358–363
- Russell MJ, Daniel RM, Hall AJ, Sherringham J (1994) A hydrothermally precipitated catalytic iron sulphide membrane as a first step toward life. *J Mol Evol* 39:231–243
- Russell MJ, Hall AJ, Martin W (2010) Serpentinization as a source of energy at the origin of life. *Geobiology* 8:355–371
- Russell MJ, Barge LM, Bhartia R, Bocanegra D, Bracher PJ, Branscomb E, Kidd R, McGlynn S, Meier DH, Nitschke W, Shibuya T, Vance S, White L, Kanik I (2014) The drive to life on wet and icy worlds. *Astrobiology* 14:308–343
- Schoonen MAA, Barnes HL (1988) An approximation of the second dissociation constant for H₂S. *Geochim Cosmochim Acta* 52:649–654
- Schrenk MO, Brazelton WJ (2013) Serpentinization, carbon, and deep life. *Rev Mineral Geochem* 75:575–606
- Seewald JS, Zolotov MY, McCullom T (2006) Experimental investigation of single carbon compounds under hydrothermal conditions. *Geochim Cosmochim Acta* 70:446–460

- Shibuya T, Komiya T, Nakamura K, Takai K, Maruyama S (2010) Highly alkaline, high-temperature hydrothermal fluids in the early Archean ocean. *Precambrian Res* 182:230–238
- Shibuya T, Yoshizaki M, Masaki Y, Suzuki K, Takai K, Russell MJ (2013) Reactions between basalt and CO₂-rich seawater at 250 and 350 °C, 500 bars: implications for the CO₂ sequestration into the modern oceanic crust and the composition of hydrothermal vent fluid in the CO₂-rich early ocean. *Chem Geol* 359:1–9
- Shock EL (1992) Stability of peptides in high-temperature aqueous solutions. *Geochim Cosmochim Acta* 56:3481–3491
- Shock EL (1995) Organic acids in hydrothermal solutions: Standard molal thermodynamic properties of carboxylic acids and estimates of dissociation constants at high temperatures and pressures. *Am J Sci* 295:496–580
- Shock E, Canovas P (2010) The potential for abiotic organic synthesis and biosynthesis at seafloor hydrothermal systems. *Geofluids* 10:161–192
- Shock EL, Helgeson HC (1990) Calculation of the thermodynamic and transport properties of aqueous species at high pressures and temperatures: standard partial molal properties of organic species. *Geochim Cosmochim Acta* 54:915–945
- Shock EL, Schulte MD (1998) Organic synthesis during fluid mixing in hydrothermal systems. *J Geophys Res* 103:28513–28527
- Shock EL, Helgeson HC, Sverjensky DA (1989) Calculation of the thermodynamic and transport properties of aqueous species at high pressures and temperatures: standard partial molal properties of inorganic neutral species. *Geochim Cosmochim Acta* 53:2157–2183
- Shock EL, Oelkers EH, Johnson JW, Sverjensky DA, Helgeson HC (1992) Calculation of the thermodynamic properties of aqueous species at high pressures and temperatures. *J Chem Soc Faraday Trans* 88:803–826
- Shock EL, Sassani DC, Willis M, Sverjensky DA (1997) Inorganic species in geologic fluids: correlations among standard molal thermodynamic properties of aqueous ions and hydroxide complexes. *Geochim Cosmochim Acta* 61:907–950
- Smith RM, Martell AE (2004) NIST critically selected stability constants of metal complexes, ver. 8; U. S. Department of Commerce, Technology Administration. U. S. Government Printing Office, Washington
- Smith ERB, Smith PK (1942) Thermodynamic properties of solution of amino acids and related substances. VIII. The ionization of glycylglycine, ϵ -aminocaproic acid, and aspartic acid in aqueous solution from one to fifty degrees. *J Biol Chem* 146:187–195
- Sorenson EC, Price JL, McRae BR, Woolley EM (2003) Thermodynamics of proton dissociations from aqueous L-proline: apparent molar volumes and apparent molar heat capacities of the protonated cationic, zwitterionic, and deprotonated anionic forms at temperatures from 278.15 to 393.15 K and at the pressure 0.35 MPa. *J Chem Thermodyn* 35:529–553
- Sverjensky DA, Shock EL, Helgeson HC (1997) Prediction of the thermodynamic properties of aqueous metal complexes to 1000 °C and 5 kb. *Geochim Cosmochim Acta* 61:1359–1412
- Takai K, Nakamura K (2011) Archaeal diversity and community development in deep-sea hydrothermal vents. *Curr Opin Microbiol* 14:282–291
- Takai K, Nakamura K, Suzuki K, Inogaki F, Neelson KH, Kumagai H (2006) Ultrafascis–Hydrothermalism–Hydrogenesis–HyperSLiME (UltraH³) linkage: a key insight into early microbial ecosystem in the Archean deep-sea hydrothermal systems. *Paleontol Res* 10:269–282
- Tanger JC, Helgeson HC (1988) Calculation of the thermodynamic and transport properties of aqueous species at high pressures and temperatures: revised equations of state for the standard partial molal properties of ions and electrolytes. *Am J Sci* 288:19–98
- Tivey MK (2007) Generation of seafloor hydrothermal vent fluids and associated mineral deposits. *Oceanography* 20:50–65
- Wang P, Oscarson JL, Gillespie SE, Izatt RM, Cao H (1996) Thermodynamics of protonation of amino acid carboxylate groups from 50 to 125 °C. *J Sol Chem* 25:243–266
- Ziemer SP, Woolley EM (2007a) Thermodynamics of proton dissociations from aqueous threonine and isoleucine at temperatures from (278.15 to 393.15) K, molalities from (0.01 to 1.0) mol·kg⁻¹, and at the pressure 0.35 MPa: apparent molar heat capacities and apparent molar volumes of zwitterionic, protonated cationic, and deprotonated anionic forms. *J Chem Thermodyn* 39:67–87
- Ziemer SP, Woolley EM (2007b) Thermodynamics of proton dissociations from aqueous L-methionine at temperatures from (278.15 to 393.15) K, molalities from (0.0125 to 1.0) mol·kg⁻¹, and at the pressure 0.35 MPa: apparent molar heat capacities and apparent molar volumes of L-methionine, methioninium chloride, and sodium methioninate. *J Chem Thermodyn* 39:493–506
- Ziemer SP, Woolley EM (2007c) Thermodynamics of the first and second proton dissociations from aqueous L-aspartic acid and L-glutamic acid at temperatures from (278.15 to 393.15) K and at the pressure 0.35 MPa: apparent molar heat capacities and apparent molar volumes of zwitterionic, protonated cationic, and deprotonated anionic forms at molalities from (0.002 to 1.0) mol·kg⁻¹. *J Chem Thermodyn* 39:645–666

- Ziemer SP, Niederhauser TL, Merkley ED, Price JL, Sorenson EC, McRae BR, Patterson BA, Origlia-Luster ML, Woolley EM (2006a) Thermodynamics of proton dissociations from aqueous glycine at temperatures from 278.15 to 393.15 K, molalities from 0 to 1.0 mol·kg⁻¹, and at the pressure 0.35 MPa: apparent molar heat capacities and apparent molar volumes of glycine, glycinium chloride, and sodium glycinate. *J Chem Thermodyn* 38:467–483
- Ziemer SP, Niederhauser TL, Merkley ED, Price JL, Sorenson EC, McRae BR, Patterson BA, Woolley EM (2006b) Thermodynamics of proton dissociations from aqueous serine at temperatures from (278.15 to 393.15) K, molalities from (0.01 up to 1.0) mol·kg⁻¹, and at the pressure 0.35 MPa: apparent molar heat capacities and apparent molar volumes of serine, serinium chloride, and sodium serinate. *J Chem Thermodyn* 38:634–648
- Ziemer SP, Niederhauser TL, Price JL, Woolley EM (2006c) Thermodynamics of proton dissociations from aqueous alanine at temperatures from (278.15 to 393.15) K, molalities from (0.0075 to 1.0) mol·kg⁻¹, and at the pressure 0.35 MPa: apparent molar heat capacities and apparent molar volumes of alanine, alanium chloride, and sodium alaninate. *J Chem Thermodyn* 38:939–951